

# Automated Detection and Diagnosis of Diabetic Retinopathy: A Comprehensive Survey

Vasudevan Lakshminarayanan<sup>1\*</sup>, Hoda Kheradfallah<sup>1</sup>, Arya Sarkar<sup>2</sup>, J. Jothi Balaji<sup>3</sup>

<sup>1</sup>Theoretical and Experimental Epistemology Lab, School of Optometry and Vision Science, University of Waterloo, Waterloo, Ontario N2L 3G1, Canada

<sup>2</sup>Department of Computer Engineering, University of Engineering and Management, Kolkata - 700 156, India

<sup>3</sup>Department of Optometry, Medical Research Foundation, Chennai - 600 006, India

\*Correspondence: [vengulak@uwaterloo.ca](mailto:vengulak@uwaterloo.ca)

## ABSTRACT

Diabetic Retinopathy (DR) is a leading cause of vision loss in the world. In the past few years, Artificial intelligence (AI) based approaches have been used to detect and grade DR. Early detection enables appropriate treatment and thus prevents vision loss. Both fundus and optical coherence tomography (OCT) images are used to image the retina. With deep learning / machine-learning-based approaches is possible to extract features from the images and detect the presence of DR. Multiple strategies are implemented to detect and grade the presence of DR using classification, segmentation, and hybrid techniques. This review covers the literature dealing with AI approaches to DR that has been published in the open literature in five-years (2016-2021). In addition, a comprehensive list of available DR datasets is reported. Both the PICO (P-Patient, I-Intervention, C-Control, O-Outcome) and Preferred Reporting Items for Systematic Review and Meta-analysis (PRISMA) 2009 search strategies were employed. We summarize a total of 114 published articles which conformed to the scope of the review. In addition, a list of 43 major datasets is presented.

**Keywords:** Diabetic Retinopathy, Artificial intelligence, Deep learning, Machine-learning, Datasets, Fundus Image, Optical coherence tomography, and Ophthalmology.

## 1. Introduction

Diabetic retinopathy (DR) is a major cause of irreversible visual impairment and blindness worldwide [1]. This etiology of DR is due to chronic high blood glucose levels which cause retinal capillary damage. DR mainly affects the working-age population and has a high prevalence rate globally, from 2.6 million in

2015 to 191 million by 2030 [2]. There are two main reasons why early detection is important, DR is difficult to detect in its early stages since there are no visual symptoms. Progression of the disease can lead to blindness. So early diagnosis and regular screening can decrease the risk of visual loss to 57.0 % as well as the cost of treatment [2] DR is clinically graded by observation of the retinal fundus either directly or through imaging techniques such as fundus photography or optical coherence tomography, There are several standard DR grading systems such as the Early Treatment Diabetic Retinopathy Study (ETDRS) grading system [3] with multiple grading levels separating fine detailed DR characteristics evaluated upon all seven retinal fundus fields of view (FOV). Although ETDRS [4] is the gold standard, due to implementation complexity and technical limitations [5], alternative systems are also used such as International Clinical Diabetic Retinopathy (ICDR) [6] scale which is accepted in both clinical and Computer-Aided Diagnosis (CAD) expand settings [7]. The ICDR scale defines 5 severity levels, 4 levels for diabetic macular edema (DME) and requires fewer FOVs [6]. The ICDR levels are discussed below and is illustrated in Fig 1.

- **No Apparent Retinopathy:** No abnormalities.
- **Mild Non-Proliferative Diabetic Retinopathy (NPDR):** This is the first stage of diabetic retinopathy, specifically characterized by tiny areas of swelling in the blood vessels of the retina known as micro aneurysms (MA) [8]. There is an absence of profuse bleeding in the retinal nerves and if DR is detected at this stage, it can help save the patients eyesight with proper medical treatment (Fig 1A)
- **Moderate NPDR:** When left unchecked, mild NPDR progresses is a moderate stage when there is leakage of blood from the blocked retinal vessels. Also, at this stage Hard Exudates (Ex) may exist (Fig 1B). The dilation and constriction of venules in the retina causes venous beading (VB) which are visible ophthalmospically [8].
- **Severe NPDR:** A larger number of blood vessels in the retina are blocked in this stage, causing over 20 intraretinal hemorrhages (IHE; Fig 1C) in all 4 retinal quadrants or there are intraretinal microvascular abnormalities (IRMA) which can be seen as bulges of thin vessels which appear small with and sharp border red spots in at least one quadrant and/or there is definite evidence of VB in over 2 quadrants [8].

- Proliferative Diabetic Retinopathy (PDR):** This is an advanced stage of the disease and occurs when the condition is left unchecked for an extended period of time. New blood vessels form in the retina and this condition is termed neovascularization (NV). These blood vessels are often fragile, with a consequent risk of fluid leakage and proliferation of fibrous tissue [8]. Different functional visual problems will occur at this stage, such as blurriness, reduced field of vision, and even complete blindness in some cases (Fig D).

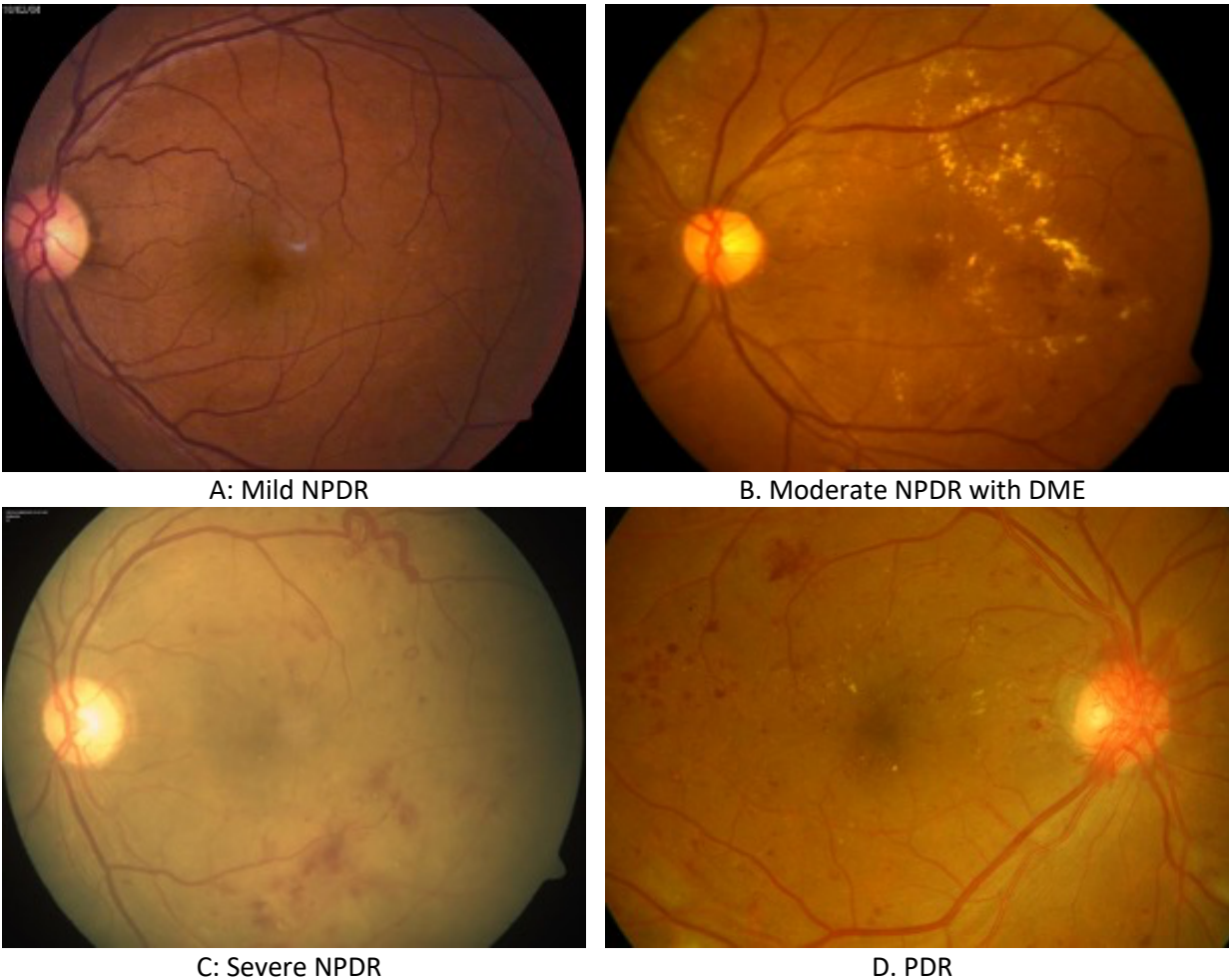


**Fig 1.** Retinal fundus images of different stages of diabetic retinopathy. (A) Stage II: Mild non-proliferative diabetic retinopathy; (B) Stage III: Moderate non-proliferative diabetic retinopathy; (C) Stage IV: Severe non-proliferative diabetic retinopathy; (D) Stage V: Proliferative diabetic retinopathy. (Images courtesy of Rajiv Raman et al. Sankara Nethralaya, India)

The fine pathognomonic DR signs in the initial stages are determined normally, after dilating pupils (mydriasis), DR screening is performed through slit lamp bio-microscopy with a +90.0 D lens, and direct [9] / indirect ophthalmoscopy to detect [10]. This procedure is time consuming, requires highly trained clinicians who have considerable experience, diagnostic precision that requires time, economic costs and

resources. Even if all these are available there is still the possibility of misdiagnosis [11]. This dependency on manual evaluation reading makes the situation more challenging. In year 2020, the number of adults worldwide with DR, and vision-threatening DR was estimated to be 103.12 million, and 28.54 million. By year 2045, the numbers are projected to increase to 160.50 million, and 44.82 million[12]. In addition, in developing countries where there is a shortage of ophthalmologist [13,14] as well as access to standard clinical facilities. This problem also exists in underserved areas of the developed world.

Recent developments in Computer-Aided Diagnosis (CAD) techniques are becoming more prominent in modern ophthalmology [15] as they can save time, cost and human resource for routine DR screening and involve lower diagnostic error factors [15]. CAD can also efficiently manage the increasing number of afflicted DR patients [16] and diagnose DR in early stages with fewer sight threatening effects. These techniques vary depending on the imaging system. The commonly applied imaging methods such as Optical Coherence Tomography (OCT), OCT Angiography (OCTA), Ultrawide-field fundus (UWF) and standard 45° fundus photography are covered in this review. The study performed by Majumder et al[15] reported a smartphone camera screening real time procedure for DR screening.

The main purpose of this review is to analyze 114 articles published within the last 6 years that focus on the detection of DR using CAD techniques. These techniques have made considerable progress in performance with the use of machine learning (ML) and deep learning (DL) schemes that employ the latest developments in deep convolutional neural networks (DCNNs) architectures for DR severity grading, progression analysis, abnormality detection and semantic segmentation. An overview of ophthalmic applications of convolutional neural networks is presented in [17,18,19,20].

## **2. Methods**

### **2.1. Literature search details**

For this review, literature from 5 publicly accessible databases were surveyed, and these databases were chosen based on their depth, their ease of accessibility, and their popularity. These 5 databases are:

- PubMed: Publications from MEDLINE (<https://pubmed.ncbi.nlm.nih.gov/>)
- IEEE Xplore: IEEE conference & journals (<https://ieeexplore.ieee.org/Xplore/home.jsp>)

- PUBLONS: Publications from Web of Science (<https://publons.com/about/home/>)
- SPIE digital library: Conference & journals from SPIE (<https://www.spiedigitallibrary.org/>)
- Google Scholar: Database containing conference and journal proceedings from multiple databases (<https://scholar.google.co.in/>).

Google Scholar has been chosen to fill the gaps in the search strategy by identifying literature from multiple sources, along with articles that might've been missed during manual selection from the other four databases. This review covers the 5-year time-period (2016-2021) so that it is current and the fact that advances in AI enabled diabetic retinopathy detection and grading during this time frame has increased considerably (Fig 2). This figure was generated using the PubMed results.

At the time of writing this review, a total of 10,635 search results were listed in the PubMed database for this time period when just the term "*diabetic retinopathy*" was used. The MEDLINE database is arguably the largest for bio-medical research and are resources from the National Library of Medicine, a part of the U.S. National Institutes of Health.

A search of the IEEE Xplore library and the SPIE digital library for the given time period and search term, report a total of 812 and 332 search results respectively. The IEEE Xplore and SPIE libraries contain only publications of these two professional societies. The other databases further added to this list by listing papers from non-traditional sources such as pre-print servers). In Fig 3 we plot the number of papers published as a function of year using data from all sources.

The scope of this review however is limited to "automated detection and grading of diabetic retinopathy using fundus & OCT images" i.e., the use of artificial intelligence, specifically deep learning, and machine learning techniques to enable detection and grading of diabetic retinopathy in fundus and OCT images. Therefore, to make the search more manageable, a combination of relevant keywords was used using the PICO (P-Patient, I-Intervention, C-Control, O-Outcome) search strategy [21]. The keywords used in the PICO search were predetermined. A combination of ("Diabetic Retinopathy" AND ("deep learning" OR "machine learning" OR "artificial intelligence")) AND (fundus OR OCT) were used which reduced the initial 10,635 search results in PubMed to just 266. during the period under consideration. A manual process of eliminating duplicate search results carried out across the results from all obtained databases resulted in a total number of 114 papers and is represented in the comprehensive.

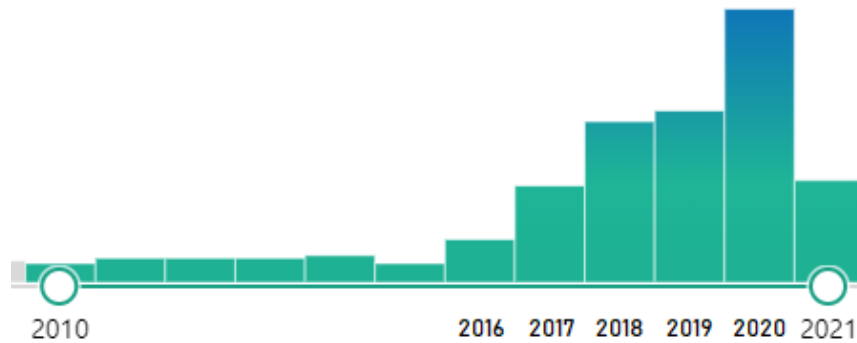


**Fig 2:** Increase in the number of articles matching the predefined keywords over the last 5 years; the PubMed search results were used to create this figure

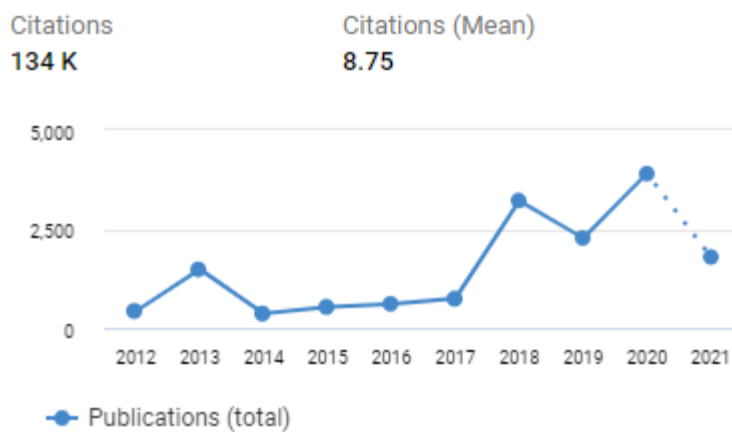


**Fig 3:** A plot of the number of articles as a function of year. This figure was generated using results from all 5 databases using search terms *Diabetic Retinopathy AND (Deep Learning OR Machine Learning)*

The search strategy for identifying relevant research for the review involved three main steps:

1. Using the predefined set of keywords and logical operators, a small set of papers were identified in this time range (2016-21).
2. Using a manual search strategy, the papers falling outside the scope of this review were eliminated.
3. The duplicate articles (i.e. the papers occurring in multiple databases) were eliminated to obtain the set of unique articles used in this review.

The search strategy followed by this review abides by the Preferred Reporting Items for Systematic Review and Meta-analysis (PRISMA) 2009 checklist [22], and the detailed search and identification pipeline is shown in Fig 4.

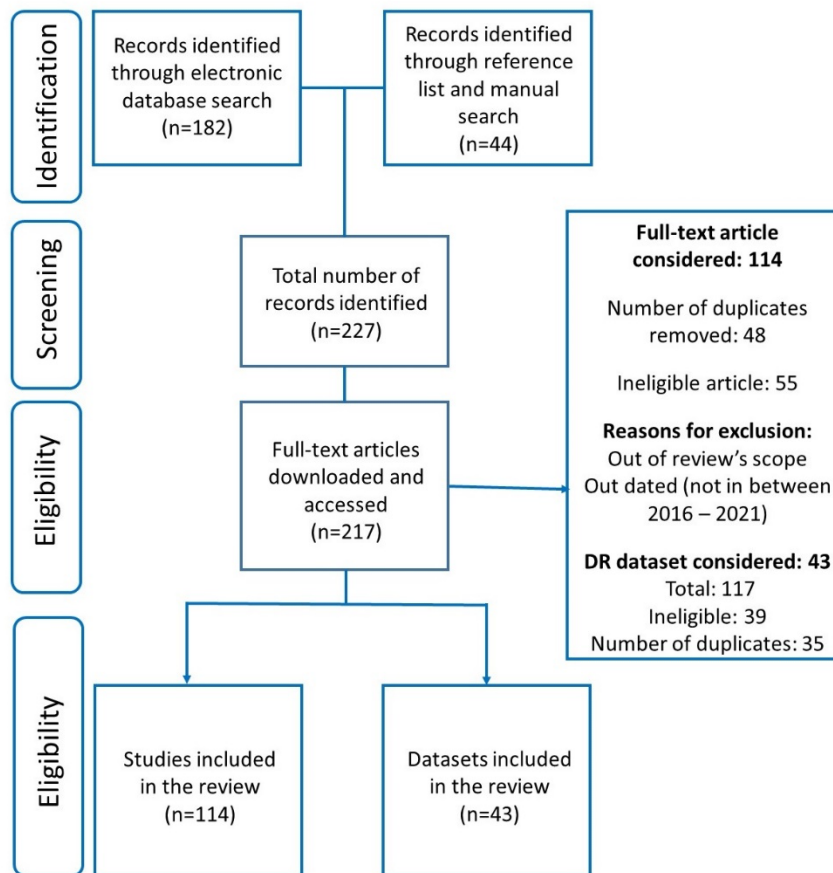


**Fig 4:** Flowchart summarizing the literature search and dataset identification using PRISMA review strategy for identifying articles related to automated detection and diagnosis of diabetic retinopathy.

## 2.2. Dataset search details

The backbone of any automated detection model, be it ML based, DL based, or multi-model-based, is the dataset used for training and validation. High-quality data, which can capture the features of the retina and are correctly graded are of extreme importance in training a good DR detection model. In this review, a comprehensive list of datasets has been created and discussed. A previously published paper[23] also gives a list of ophthalmic image datasets, containing 33 datasets that can be used for training DR detection and grading models. The paper by Khan et al 2021 [23] highlighted 33 of the 43 datasets presented in Table 1. However, some databases which are popular and publicly accessible are not listed by Khan et al 2021 [23] e.g. (UoA-DR [24], Longitudinal DR screening data [25], FGADR [26] etc.), We have identified additional datasets that are available for use.

The search strategy for determining relevant DR detection datasets is as follows:

1. Appropriate results from all 5 of the selected databases (PubMed, PUBLONS, etc.) were searched manually so gather information about names of datasets for DR detection and grading.
2. The original papers and websites associated with each dataset were analyzed and a systematic, tabular representation of all available information was created.
3. The Google dataset search and different forums were checked for missing dataset entries and STEP-2 was repeated for all original datasets found.
4. A final comprehensive list of datasets and its details was generated and represented in Table 1.

A total of 43 datasets were identified employing the search strategy given above. Upon further inspection, a total number of 30 datasets were identified as open access (OA) i.e., can be accessed easily without any permission or payment. Of the total number of datasets, 6 datasets were restricted, however the databases can be accessed with the permission of the author or institution the remaining 7 datasets were private and can't be accessed. These datasets can be used to create a generalized model because of the diversity of images (multi-national, and multi-ethnic groups).

### **3. Results**

#### **3.1. Dataset search results**

This section provides a high-level overview of the search results that were obtained using the datasets as well as, different review articles on datasets in the domain of ophthalmology e.g. Khan et al 2020 [23] and as well as different leads obtained from GitHub and other online forums. In this review, 43 datasets were identified and a general overview of the datasets is systematically presented in this section. The datasets reviewed in this article does not limit to 2016 to 2021 and can be released before that. The list of datasets and their characteristics are shown in Table 1 below. Depending on the restrictions and other proforma required for accessing the datasets, the list has been divided into 3 classes, they are:

- Public open access (OA) datasets with some having high quality DR grading,
- High-quality DR datasets, that can be accessed upon request i.e. can be accessed by filling necessary agreements and forms for fair usage, they are a sub-type of (OA) databases and are termed as access upon request (AUR) in the table.
- Private datasets from different institutions that are not publicly accessible or require explicit permission can access are termed as Not Open Access (NOA).

Table 1: Datasets for DR detection, grading and segmentation and their respective characteristics.

Dataset	No. of image	Device used	Access	Country	Year	No. Of subjects	Type	Format	Remarks
DRIVE [27]	40	Canon CR5 non-mydiatic 3CCD camera with a 45° FOV	OA	Netherlands	2004	400	Fundus	JPEG	Retinal vessel segmentation and ophthalmic diseases
DIARETDB0 [28]	130	50° FOV DFC	OA	Finland	2006	NR	Fundus	PNG	DR detection and grading
DIARETDB1 [29]	89	50° FOV DFC	OA	Finland	2007	NR	Fundus	PNG	DR detection and grading
National Taiwan University Hospital[30]	30	Heidelberg retina tomography with Rostock corneal module	OA	Japan	2007-2017	30	Fundus	TIFF	DR, pseudo exfoliation
HEI-MED [31]	169	Visucam PRO fundus camera (Zeiss, Germany)	OA	USA	2010	910	Fundus	JPEG	DR detection and grading
19 CF[32]	60	NR	OA	Iran	2012	60	Fundus	JPEG	DR detection
FFA Photographs & CF [33]	120	NR	OA	Iran	2012	60	FFA	JPEG	DR grading and lesion detection
Fundus Images with Exudates [34]	35	NR	OA	Iran	2012	NR	Fundus	JPEG	Lesion detection
DRiDB [35]	50	Zeiss VISUCAM 200 DFC at a 45° FOV	AUR	Croatia	2013	NR	Fundus	BMP files	DR grading
eOphtha [36]	463	NR	OA	France	2013	NR	Fundus	JPEG	Lesion detection
Longitudinal DR screening data [25]	1120	Topcon TRC-NW65 with a 45 degrees field of view	OA	Netherlands	2013	70	Fundus	JPEG	DR grading
22 HRF [37]	45	CF-60UVi camera (Canon)	OA	Germany and Czech Republic	2013	45	Fundus	JPEG	DR detection
RITE [38]	40	Canon CR5 non-mydiatic 3CCD camera with a 45°FOV	AUR	Netherlands	2013	Same As Drive	Fundus	TIFF	Retinal vessel segmentation and ophthalmic diseases
DR1[39]	1077	TRC-50X mydiatic camera Topcon	OA	Brazil	2014	NR	Fundus	TIFF	DR detection
DR2 [39]	520	TRC-NW8 retinography (Topcon) with a D90 camera (Nikon, Japan)	OA	Brazil	2014	NR	Fundus	TIFF	DR detection
DRIMDB [40]	216	CF-60UVi fundus camera (Canon)	OA	Turkey	2014	NR	Fundus	JPEG	DR detection and grading
FFA Photographs [41]	70	NR	OA	Iran	2014	70	FFA	JPEG	DR grading and Lesion detection
MESSIDOR 1 [42]	1200	Topcon TRC NW6 non-mydiatic retinography, 45° FOV	OA	France	2014	NR	Fundus	TIFF	DR and DME grading
Lotus eyecare hospital [43]	122	Canon non-mydiatic Zeiss fundus camera 90° FOV	NOA	India	2014	NR	Fundus	JPEG	DR detection
Srinivasan [44]	3231	SD-OCT (Heidelberg Engineering, Germany)	OA	USA	2014	45	OCT	TIFF	DR detection and grading, DME, AMD
EyePACS [45]	88,702	Centervue DRS (Centervue, Italy), Optovue iCam (Optovue, USA), Canon CR1/DGi/CR2 (Canon), and Topcon NW (Topcon)	OA	USA	2015	NR	Fundus	JPEG	DR grading
Rabbbani [46]	24 images & 24 videos	Heidelberg SPECTRALIS OCT HRA system	OA	USA	2015	24	OCT	TIFF	Diabetic Eye diseases
DR HAGIS[47]	39	TRC-NW6s (Topcon), TRC-NW8 (Topcon), or CR-DGi fundus camera (Canon)	OA	UK	2016	38	Fundus	JPEG	DR, HT, AMD and Glaucoma
JICHI DR [48]	9939	AFC-230 fundus camera (Nidek)	OA	Japan	2017	2740	Fundus	JPEG	DR grading

Rotterdam Ophthalmic Data Repository DR [49]	1120	TRC-NW65 non-mydratric DFC (Topcon)	OA	Netherlands	2017	70	Fundus	PNG	DR detection
Singapore National DR Screening Program [50]	4,94,661	NR	NOA	Singapore	2017	14 880	Fundus	JPEG	DR, Glaucoma and AMD
IDRID [51]	516	NR	OA	India	2018	NR	Fundus	JPEG	DR grading and lesion segmentation
OCTID [52]	500+	Cirrus HD-OCT machine (Carl Zeiss Meditec) Zeiss VISUCAM 500 Fundus Camera FOV	OA	Multi ethnic	2018	NR	OCT	JPEG	DR, HT, AMD
UoA-DR [53]	200	45°	AUR	India	2018	NR	Fundus	JPEG	DR grading
APTOS [54]	5590	DFC	OA	India	2019	NR	Fundus	PNG	DR grading
CSME [55]	1445	NIDEK non-mydratric AFC-330 auto-fundus camera	NOA	Pakistan	2019	NR	Fundus	JPEG	DR grading
OCTAGON [56]	213	DRI OCT Triton (Topcon)	AUR	Spain	2019	213	OCTA	JPEG & TIFF	DR detection
ODIR-2019 [57]	8000	Fundus camera (Canon), Fundus camera (ZEISS), and Fundus camera (Kowa)	OA	China	2019	5000	Fundus	JPEG	DR, HT, AMD and Glaucoma
OIA-DDR [58]	13,673	NR	OA	China	2019	9598	NR	JPEG	DR grading and lesion segmentation
Zhongshan Hospital and First People's Hospital [59]	19,233	Multiple colour fundus camera	NOA	China	2019	5278	Fundus	JPEG	DR grading and lesion segmentation
AGAR300 [60]	300	45° FOV	OA	India	2020	150	Fundus	JPEG	DR grading and MA detection
Bahawal Victoria Hospital [55]	2500	Vision Star, 24.1 Megapixel Nikon D5200 camera	NOA	Pakistan	2020	500	Fundus	JPEG	DR grading
Retinal Lesions [61]	1593	Selected from EPACS dataset	AUR	China	2020	NR	Fundus	JPEG	DR grading and lesion segmentation
Dataset of fundus images for the study of DR [62]	757	Visucam 500 camera of the Zeiss brand	OA	Paraguay	2021	NR	Fundus	JPEG	DR grading
FGADR [58]	2842	NR	OA	UAE	2021	NR	Fundus	JPEG	DR and DME grading
Optos Dataset (Tsukazaki Hospital) [63]	13047	200 Tx ultra-wide-field device (Optos, UK)	NOA	Japan	NR	5389	Fundus	JPEG	DR, Glaucoma, AMD, and other eye diseases
MESSIDOR 2 [64]	1748	Topcon TRC NW6 non-mydratric retinography 45° FOV	AUR	France	NR	874	Fundus	TIFF	DR and DME grading
Noor hospital [65]	4142	Heidelberg SPECTRALIS SD-OCT imaging system	NOA	Iran	NR	148	OCT	TIFF	DR detection

DFC: Digital fundus camera, RFC: Retinal Fundus Camera, FFA: Fundus Fluorescein Angiogram, DR: Diabetic retinopathy, MA: Microaneurysms, DME: Diabetic Macular Edema, FOV: field-of-view, AMD: Age-related Macular Degeneration; OA: Open access  
AUR: Access upon request; NOA: Not Open access; CF: Colour Fundus; HT: Hypertension; NR: Not Represented

### 3.2. Diabetic retinopathy classification

This section discusses the classification approaches used for DR detection. The classification can be for the detection of DR [66], referable DR (RDR) [67,68], vision threatening DR (vtDR) [68] or analyze the

proliferation level of DR using the ICDR system. Some studies also consider Diabetic Macular Edema (DME) [67,69]. Recent ML and DL methods have produced promising results in automated DR diagnosis. Thus, multiple performance metrics such as accuracy (ACC), sensitivity (SE) or recall, specificity (SP) or precision, area under the curve (AUC), F1 score and Kappa score are used to evaluate the classification performance. Table 2, 3 present the brief overview on articles that use fundus images for DR classification and articles that classify using novel preprocessing technique. Table 4 lists the recent DR classification studies that use OCT and OCTA images. In the following subsections we provide the details of ML and DL aspects and evaluate the performance of prior studies in terms of quantitative metrics.

### **3.2.1. Machine learning approaches**

In this review, 9 out of 93 classification-based studies employed machine learning approaches and 1 article used un-ML method for detecting and grading DR. Hence, in this section, we present the evaluation over various ML based feature extraction and decision making that have been employed in the selected primary studies to construct the DR detection models. In general, six major distinct machine learning algorithms were used in these studies such as feature extraction tools in pre-processing. These are: principal component analysis (PCA) [70,71], linear discriminant analysis (LDA)-based feature selection [71], spatial invariant feature transform (SIFT) [71], support-vector-machine (SVM) [16,71,72,73], KNN [72] and Random Forest (RF) [74]. The methods in combination with DL networks improved the performance and training process. In addition to the widely used ML methods, some studies such as [75] presented a pure ML model with an accuracy of over 80 % including distributed Stochastic Neighbor Embedding (t-SNE) for image dimensionality reduction in combination with ML Bagging Ensemble Classifier (ML-BEC) to improve classification performance using feature bagging technique with low computational time. Ali et al 2020 [55] focused on five fundamental ML models named sequential minimal optimization (SMO), logistic (Lg), multi-layer perceptron (MLP), logistic model tree (LMT), and simple logistic (SLg) in the classification level. This study proposed a novel preprocessing process in which the lesion Region of Interest (ROI) is segmented with a clustering-based method K-Means and extract features of histogram, wavelet, grey scale co-occurrence and run-length matrixes (GLCM and GLRLM) from segmented ROIs. This method outperformed previous models with an average accuracy of 98.83 % with the five ML models. However, a ML model such as SLg performs well, the required classification time is 0.38 with Intel Core i3 1.9 gigahertz (GHz) CPU, 64-bit Windows 10 operating system and 8 gigabytes (GB) memory. This processing time is higher than previous studies. We can also use ML method for OCT and

OCTA for DR detection. Recently LiU et al 2021 [76] deployed four ML models of logistic regression (LR), logistic regression regularized with the elastic net penalty (LR-EN), support vector machine (SVM), and the gradient boosting tree named XGBoost with over 246 OCTA wavelet features and obtained ACC, SE and SP of 82 %, 71 % and 77 % respectively. This study, despite inadequate results, has the potential to reach higher scores using model optimization and fine-tuning hyper parameters. These studies show a lower overall performance if using a small number of feature types and simple ML models are used. Dimensionality reduction is an application of ML models which can be added in the decision layer of CAD systems [77,78]. In a support vector machine is used for the classification of features obtained from the state of art DNNs that are optimized with PCA [78]. This provided an accuracy of 85.7 % on preprocessed images. In comparison with methods such as AlexNet, VGG, ResNet, and Inception-v3, the authors report an ACC of 99.5 %. In addition, they also found that this technique is more applicable with considerably less computational cost.

### **3.2.2. Deep learning approaches**

This section gives an overview of deep learning algorithms that have been used. Depending on the imaging system used, the image resolution, noise level, contrast as well as the size of the dataset the methods can vary. Some studies propose a customized network such as the work done by Gulshan et al 2016[67], Gargeya et al 2017[66], Rajalakshmi et al 2018[79], Riaz et al 2020[80]. These networks have lower performance outcomes than the state of art networks such as VGG, ResNet, Inception and DenseNet but the fewer layers make them more generalized, suitable for training with small datasets and computationally efficient. Quellec et al 2017 [81] applied L2 regularization over the best performed DCNN in the KAGGLE competition for DR detection named o-O. Another example is that proposed by Sayres et al 2019 [82] which showed 88.4 %, 91.5 %, 94.8 % for ACC, SE and SP respectively over a small subset of 2000 images obtained from the EyePACS database. However, the performance of this network is lower than the results obtained from Mansour et al 2018[71] which used a larger subset of the EyePACS images (35,126 images). Mansour et al 2018[71] also deployed more complex architectures such as the AlexNet on the extracted features of LDA and PCA that generated better results than Sayres et al 2019 [82] with 97.93 %, 100 % and 93 % ACC, SE and SP respectively. Such DCNNs should be used with large datasets since the large number of images used in the training reduces errors. In a deep architecture is applied for a small number of observations it might cause overfitting in which the performance over the test data is not as well as expected on the training data. On the other hand, the deepness of networks does not always

guarantee higher performance meaning that they might face with the problems such as vanishing or exploding gradient which will have to be addressed by redesigning the network to simpler architectures. Furthermore, the deep networks extract several low and high-level features. As these image features get more complicated it becomes more difficult to interpret. Sometimes these high-level attributes are not clinically meaningful. For instance, the high-level attributes may refer to an existing bias in all images belonging to a certain class such as light intensity and similar vessel patterns that is not considered as a sign of DR but the DCNN will treat it as a critical feature. Consequently, this fact makes the output prediction erroneous.

In the scope of DL-based classification [83] designed a DL model named Trilogy of Skip-connection Deep Networks (Tri-SDN) over the pretrained base model ResNet50 that applies skip connection blocks to make the tuning faster yielding to ACC and SP of 90.6 % and 82.1 % respectively, which is considerably higher than the values of 83.3 % and 64.1 % compared with skip connection blocks are not used.

There are additional studies that do not focus on proposing new network architecture but enhance the preprocessing output. The study done by Pao et al 2020[84] presents bi-channel customized CNN in which the enhanced image using an image enhancement technique known as unsharp mask and with entropy images used as the inputs of a CNN with 4 convolutional layers with results of 87.83 %, 77.81 %, 93.88 % over ACC, SE and SP. These results are all higher than the case of analysis without preprocessing (81.80 % 68.36 %, 89.87 % respectively).

Shankar et al 2020[85] proposed another approach to preprocessing using Histogram-based segmentation to extract regions containing lesions on fundus images. As the classification step this article utilized Synergic DL (SDL) model and the results indicated that the presented SDL model offers better results than popular DCNNs using MESSIDOR 1 in terms of ACC, SE, SP.

Furthermore, classification is not limited to the DR detection and DCNNs can be applied to detect the presence of DR-related lesions such as that reported by Wang et al 2020 covering twelve lesions: MA, IHE, superficial retinal hemorrhages (SRH), Ex, CWS, venous abnormalities (VAN), IRMA, NV at the disc (NVD), NV elsewhere (NVE), pre-retinal FIP, VPHE, and tractional retinal detachment (TRD) with average precision and AUC 0.67 and 0.95 respectively, however features such as VAN has low individual detection accuracy. This study provides essential steps for DR detection based on the presence of lesions that is more interpretable than DCNNs which act as black boxes [86,87,88].

There are explainable backpropagation-based methods that produce heatmaps of the lesions affecting the classifications DR such as the study done by Keel et al 2019 [89] which highlights Ex, HE and vascular abnormalities in the DR diagnosed images. These methods have limited performance providing generic explanations which might be inadequate to be clinically reliable. Tables 2, 3 and 4 briefly illustrates the previous studies in the scope of DR classification with deep methods.

Table 2: Classification-based studies in DR detection using fundus imaging.

Author, Year	Dataset	Grading details	Pre-processing	Method	Accuracy	Sensitivity	Specificity	AUC
Abramoff, 2016 [68]	MESSIDOR 2	Detect RDR and vtDR	No	DCNN: IDx-DR X2.1. ML: RF	NA	96.80%	87.00%	0.98
Chandrasekhar, 2016 [90]	EyePACS, DRIVE, STARE	Grade DR based on ICDR scale	Yes	DCNN	STARE and DRIVE: 94%	NA	NA	NA
Colas, 2016 [91]	EyePACS	Grade DR based on ICDR scale	No	DCNN	NA	96.20%	66.60%	0.94
Gulshan, 2016 [67]	EyePACS, MESSIDOR 2	Detect DR based on ICDR scale, RDR and referable DME	Yes	DCNN	NA	EyePACS: 97.5%	EyePACS: 93.4%	EyePACS: 0.99
Wong, 2016 [92]	EYEPAACS, MESSIDOR 2	Detect RDR, Referable DME (RDME)	No	DCNN	NA	90%	98%	0.99
Gargeya, 2017 [66]	EyePACS, MESSIDOR 2, eOphtha	Detect DR or non-DR	Yes	DCNN	NA	EyePACS: 94%	EyePACS: 98%	EyePACS: 0.97
Somasundaram, 2017[75]	DIARETDB1	Detect PDR, NPDR	No	ML: t-SNE and ML-BEC	NA	NA	NA	NA
Takahashi, 2017 [48]	Jichi Medical University	Grade DR with the Davis grading scale (NPDR, severe DR, PDR)	No	DCNN: Modified GoogLeNet	81%	NA	NA	NA
Ting, 2017 [30]	SiDRP	Detect RDR, vtDR, glaucoma, AMD	No	DCNN	NA	RDR: 90.5% vtDR: 100%	RDR: 91.6% vtDR: 91.1%	RDR: 0.93 vtDR: 0.95
Quellec, 2017 [81]	EyePACS, eOphtha, DIARETDB 1	Grade DR based on ICDR	Yes	DCNN: L2-regularized o-O DCNN	NA	94.60%	77%	0.955
Wang, 2017 [93]	EyePACS, MESSIDOR 1	Grade DR based on ICDR scale	Yes	Weakly supervised network to classify image and extract high resolution image patches containing a lesion	MESSIDOR 1: RDR: 91.1%	NA	NA	MESSIDOR 1: RDR: 0.957
Benson, 2018 [94]	Vision Quest Biomedical database	Grade DR based on ICDR scale + scars detection	Yes	DCNN: Inception v3	NA	90%	90%	0.95.
Chakrabarty, 2018 [95]	High-Resolution Fundus (HRF) Images	Detect DR	Yes	DCNN	91.67%	100%	100%	F1 score: 1
Costa, 2018 [96]	MESSIDOR 1	Grade DR based on ICDR scale	No	Multiple Instance Learning (MIL)	NA	NA	NA	0.9

Dai, 2018 [97]	DIARETDB1	MA, HE, CWS, Ex detection	Yes	DCNN: Multi-sieving CNN(image to text mapping)	96.10%	87.80%	99.70%	F1 score: 0.93
Dutta, 2018 [98]	EyePACS	Mild NPDR, Moderate NPDR, Severe NPDR, PDR	Yes	DCNN: VGG-Net	86.30%	NA	NA	NA
Kwasigroch, 2018 [99]	EyePACS	Grade DR based on ICDR scale	Yes	DCNN: VGG D	81.70%	89.50%	50.50%	NA
Levenkova, 2018 [77]	UWF (Ultra-Wide Field)	Detect CWS, MA, HE, Ex	No	DCNN, SVM	NA	NA	NA	0.80
Mansour, 2018 [71]	EyePACS	Grade DR based on ICDR scale	Yes	DCNN, ML: AlexNet, LDA, PCA, SVM, SIFT	97.93%	100%	0.93	NA
Rajalakshmi, 2018 [7]	Smartphone-based imaging device	Detect DR and vtDR Grade DR based on ICDR scale	No	DCNN	NA	DR: 95.8% vtDR: 99.1%	DR: 80.2% vtDR: 80.4%	NA
Robiul Islam, 2018 [100]	APTOS 2019	Grade DR based on ICDR scale	Yes	DCNN: VGG16	91.32%	NA	NA	NA
Zhang, 2018 [101]	EyePACS	Grade DR based on ICDR scale	Yes	DCNN: Resnet-50	NA	61%	84%	0.83
Zhang, 2018 [102]	EyePACS	Grade DR based on ICDR scale	No	DCNN	82.10%	76.10%	0.855	Kappa score: 0.66
Arcadu, 2019 [103]	7 FOV images of RIDE and RISE datasets	2 step grading based on ETDRS	No	DCNN: Inception v3	NA	66%	77%	0.68
Bellemo, 2019 [104]	Kitwe Central Hospital, Zambia	Grade DR based on ICDR scale	No	DCNN: Ensemble of Adapted VGGNet & Resenet	NA	RDR: 92.25% vtDR: 99.42%	RDR: 89.04%	RDR: 0.973 vt DR: 0.934
Chowdhury, 2019 [105]	EyePACS	Grade DR based on ICDR scale	Yes	DCNN: Inception v3	2 Class: 61.3%	NA	NA	NA
Govindaraj, 2019 [106]	MESSIDOR 1	Detect DR	Yes	Probabilistic Neural Network	98%	Almost 90% from chart	Almost 97% from chart	F1 score: almost 0.97
Gulshan, 2019 [107]	Aravind Eye Hospital and Sankara Nethralaya, India	Grade DR based on ICDR scale	No	DCNN	NA	Aravind: 88.9% SN: 92.1%	Aravind: 92.2% SN: 95.2%	Quadratic weighted K scores: Aravind: 0.85 SN: 0.91
Hathwar, 2019 [108]	EyePACS, IDRID	Detect DR	Yes	DCNN: Xception-TL	NA	94.30%	95.50%	Kappa score: 0.88
He, 2019 [109]	IDRID	Detect DR grade and DME risk	Yes	DCNN: AlexNet	DR grade: 65%	NA	NA	NA
Hua, 2019 [83]	Kyung Hee University Medical Center	Grade DR based on ICDR scale	No	DCNN: Tri-SDN	90.60%	96.50%	82.10%	0.88
Jiang, 2019 [110]	Beijing Tongren Eye Center	DR or Non-DR	Yes	DCNN: Inception v3, Resnet152 and Inception-Resnet- v2	Integrated model: 88.21%	Integrated model: 85.57%	Integrated model: 90.85%	0.946
Li, 2019 [111]	IDRID, MESSIDOR 1	Grade DR based on ICDR scale	No	DCNN: Attention network based on ResNet50	DR: 92.6%, DME: 91.2%	DR: 92.0%, DME: 70.8%	NA	DR: 0.96 DME: 0.92
Li, 2019 [59]	Shanghai Zhongshan Hospital (SZH) and Shanghai First People's Hospital (SFPH), China, MESSIDOR 2	Grade DR based on ICDR scale	Yes	DCNN: Inception v3	93.49%	96.93%	93.45%	0.9905

Metan, 2019 [112]	EyePACS	Grade DR based on ICDR scale	Yes	DCNN: Res-Net	81%	NA	NA	NA
Nagasawa, 2019 [113]	Saneikai Tsukazaki Hospital and To-kushima University Hospital, Japan	Detect PDR	Yes	DCNN: VGG-16	NA	PDR:94.7%	PDR:97.2%	PDR: 0.96
Qummar, 2019 [114]	EyePACS	Grade DR based on ICDR scale	Yes	DCNN: Ensemble of (Resnet50, Inceptionv3, Xception, Dense121, Dense169)	80.80%	51.50%	86.72%	F1 score: 0.53
Ruamviboonsuk, 2019 [115]	Thailand national DR screening program dataset	Grade DR based on ICDR and detect RDME	No	DCNN	NA	DR: 96.8%	DR: 95.6%	DR: 0.98
Sahlsten, 2019 [69]	Private dataset	Detect DR based on multiple grading systems, RDR and DME	Yes	DCNN: Inception-v3	NA	89.60%	97.40%	0.98
Sayres, 2019 [82]	EyePACS	Grade DR based on ICDR	No	DCNN	88.40%	91.50%	94.80%	NA
Sengupta, 2019 [116]	EyePACS, MESSIDOR 1	Grade DR based on ICDR scale	Yes	DCNN: Inception-v3	90.4%	90%	91.94%	NA
Ting, 2019 [117]	SIDRP, SIMES, SINDI, SCES, BES, AFEDS, CUHK, DMP Melb, with 2 FOV	Grade DR based on ICDR scale	Yes	DCNN	NA	NA	NA	Detect DR: 0.86 RDR: 0.96
Zeng, 2019 [118]	EyePACS	Grade DR based on ICDR scale	Yes	DCNN: Inception v3	NA	82.2 %	70.7 %	0.95
Ali, 2020 [55]	Bahawal Victoria Hospital, Pakistan.	Grade DR based on ICDR scale	Yes	ML: SMO, Lg, MLP, LMT, Lg employed on selected post-opti-mized hybrid feature datasets	MLP: 73.73% LMT: 73.00 SLg: 73.07 SMO: 68.60 Lg: 72.07%	NA	NA	MLP: 0.916 LMT: 0.919 SLg: 0.921 SMO: 0.878 Lg: 0.923
Araujo, 2020 [119]	EyePACS, MESSIDOR 2, IDRID, DMR, SCREEN-DR, DR1, DRIMDB, HRF	Grade DR based on ICDR scale	Yes	DCNN	NA	NA	NA	Kappa score: EyePAC:0.74 98.60%
Chetoui, 2020 [24]	EyePACS, MESSIDOR 1, 2, eOphta, UoA-DR from the University of Auckland research, IDRID, STARE, DI-ARETDBO, 1	Grade DR based on ICDR scale	Yes	DCNN: Inception-ResNet v2	97.90%	95.80%	97.10%	98.60%
Elsawah, 2020 [73]	IDRID	Grade DR based on ICDR scale	Yes	DCNN: Res-Net 50 + NN or SVM	NN: 88% SVM: 65% 97%	NA	NA	NA
Gadekallu, 2020 [70]	DR Debrecen dataset collection of 20 features of MESSIDOR 1	DR or Non-DR	Yes	DCNN ML: PCA+Firefly	97.30%	92%	95%	NA
Gadekallu, 2020 [120]	DR Debrecen dataset	Detect DR	Yes	ML: PCA+ grey wolf optimization (GWO)+ DNN	97.30%	91%	97%	NA
Gayathri, 2020 [121]	MESSIDOR 1, EyePACS, DIARETDBO	Grade DR based on ICDR scale	NA	Wavelet Transform, SVM, RF	MESSIDOR 1: 99.75%	MESSIDOR 1: 99.8%	MESSIDOR 1: 99.9%	NA
Jiang, 2020 [122]	MESSIDOR 1	Image-wise label the presence of MA, HE, Ex, CWS	Yes	DCNN: Res-Net 50 based	MA: 89.4% HE: 98.9% Ex: 92.8% CWS: 88.6% Normal: 94.2%	MA: 85.5% HE: 100% Ex: 93.3% CWS: 94.6% Normal: 93.9%	MA: 90.7% HE: 98.6% Ex: 92.7% CWS: 86.8% Normal: 94.4%	MA: 0.94 HE: 1 Ex: 0.97 CWS: 0.97 Normal: 0.98

Lands, 2020 [123]	APTOS 2019, APTOS 2015	Grade DR based on ICDR scale	Yes	DCNN: DensNet 169	93%	NA	NA	Kappa score: 0.8
Ludwig, 2020 [10]	EyePACS, APTOS, MESSIDOR 2, EYEGO	Detect RDR	Yes	DCNN: DenseNet201	NA	MESSIDOR 2: 87%	MESSIDOR 2: 80%	MESSIDOR 2: 0.92 NA
Majumder, 2020 [15]	EyePACS, APTOS 2019	Grade DR based on ICDR scale	Yes	CNN	88.50%	NA	NA	NA
Memari, 2020 [124]	MESSIDOR 1, HEI-MED	Detect DR	Yes	DCNN	NA	NA	NA	NA
Narayanan, 2020 [78]	APTOS 2019	Detect and grade DR based on ICDR scale	Yes	DCNN: AlexNet, ResNe, VGG16, Inception v3	98.4%	NA	NA	0.985
Pao, 2020 [84]	EyePACS	Grade DR based on ICDR scale	Yes	CNN: bichannel customized CNN	87.83%	77.81%	93.88%	0.93
Paradisa, 2020 [72]	DIARETDB 1	Grade DR based on ICDR scale	Yes	ResNet-50 for extraction and SVM, RF, KNN, and XGBoost as classifiers	SVM: 99%, KNN: 100%	SVM: 99%, KNN: 100%	NA	NA
Patel, 2020 [125]	EyePACS	Grade DR based on ICDR scale	Yes	DCNN: MobileNet v2	91.29%	NA	NA	NA
Riaz, 2020 [80]	EyePACS, MESSIDOR 2	NA	Yes	DCNN	NA	EyePACS: 94.0%	EyePACS: 97.0%	EyePACS: 0.98 NA
Samanta, 2020 [126]	EyePACS	Grade DR based on ICDR scale	Yes	DCNN: DenseNet121 based	84.1 %	NA	NA	NA
Serener, 2020 [127]	EyePACS, MESSIDOR 1, eOphta, HRF, IDRID	Grade DR based on ICDR scale	Yes	DCNN: ResNet 18	Country: EyePACS: 65% Continent: EyePACS+HRF: 80%	Country: EyePACS: 17% Continent: EyePACS+HRF: 80%	Country: EyePACS: 89% Continent: EyePACS+HRF: 80%	NA
Shaban, 2020 [128]	APTOS	Grade DR to non-DR, moderate DR, and severe DR	Yes	DCNN	88%	87%	94%	0.95
Shankar, 2020 [85]	MESSIDOR 1	Grade DR based on ICDR scale	Yes	DCNN: Histogram-based segmentation+SDL	99.28%	98.54%	99.38%	NA
Singh, 2020 [129]	IDRID, MESSIDOR 1	Grade DME in 3 levels	Yes	DCNN: Hierarchical Ensemble of CNNs (HE-CNN)	96.12%	96.32%	95.84%	F1 score: 0.96
Thota, 2020 [130]	EyePACS	NA	Yes	DCNN: VGG16	74%	80.0 %	65.0 %	0.80
Wang, 2020 [131]	2 Eye hospitals, DIARETDB1, EyePACS, IDRID	MA, HE, EX	Yes	DCNN	MA: 99.7% HE: 98.4% EX: 98.1% Grading: 91.79%	Grading: 80.58%	Grading: 95.77%	Grading: 0.93
Wang, 2020 [132]	Shenzhen, Guangdong, China	Grade DR severity based on ICDR scale and detect MA, IHE, SRH, HE, CWS, VAN, IRMA, NVE, NVD, PFP, VPH, TRD	No	DCNN: Multi-task network using channel-based attention blocks	NA	NA	NA	Kappa score: 0.80 Grading: 0.64 DR feature: 0.64 F1 score: 0.93
Zhang, 2020 [133]	3 Hospitals in China	Classify to retinal tear & retinal detachment, DR and pathological myopia	Yes	DCNN: InceptionResNetv2	93.73%	91.22%	96.19%	F1 score: 0.93
Abdelmaksou	EyePACS, MESSIDOR 1, eOphta, CHASEDB 1,		Yes	U-Net + SVM	95.10%	86.10%	86.80%	0.91

d , 2021 [134]	HRF, IDRID, STARE, DIARETDB0,1								
Bora, 2021 [115]	EyePACS	Grade DR based on ICDR scale	No	DCNN: Inception v3	NA	NA	NA	Three FOV: 0-79 One FOV: 0-70	
Gangwar, 2021 [135]	APTOS 2019, MESSIDOR 1	Grade DR based on ICDR scale	Yes	DCNN: Inception ResNet v2	AP-TOS:82.18% MESSIDOR 1: 72.33%	NA	NA	NA	
He, 2021 [136]	DDR, MESSIDOR 1, EyePACS	Grade DR based on ICDR scale	No	DCNN: MobileNet 1 with attention blocks	MESSIDOR 1: 92.1%	MESSIDOR 1: 89.2%	MESSIDOR 1: 91%	F1 score: MESSIDOR 1: 0.89	
Hsieh,2021 [30]	National Taiwan University Hospital (NTUH) , Taiwan, EyePACS	Detect any DR, RDR and PDR	Yes	DCNN: Inception v4 for any DR and RDR and ResNet for PDR	Detect DR: 90.7% RDR: 90.0% PDR: 99.1% 85%	Detect DR: 92.2% RDR: 99.2% PDR: 90.9%	Detect DR: 89.5% RDR: 90.1% PDR: 99.3%	0.955	
Khan, 2021[137]	EyePACS	Grade DR based on ICDR scale	Yes	DCNN: customized highly nonlinear scale-invariant network	83.38%	55.6 %	91.0 %	F1 score: 0.59	
Oh , 2021 [2]	7 FOV fundus images of Catholic Kwandong University, South Korea	Detect DR	Yes	DCNN: ResNet 34	83.38%	83.38%	83.41%	0.915	
Saeed, 2021 [138]	MESSIDOR, EyePACS	Grade DR based on ICDR scale	No	DCNN: ResNet GB	EyePACS: 99.73%	EyePACS: 96.04%	EyePACS:99.81%	EyePACS: 0.98	
Wang, 2021 [139]	EyePACS, images from Peking Union Medical College Hospital, China	Detect RDR with lesion-based segmentation of PHE, VHE, NV, CWS, FIP, IHE, IRMA and MA, then staging based on ICDR scale	No	DCNN: Inception v3	NA	EyePACS: 90.60%	EyePACS: 80.70%	EyePACS: 0.943	
Wang. 2021 [140]	MESSIDOR 1	Grade DR based on ICDR scale	Yes	DCNN: Multi-channel-based GAN with semi supervision	RDR: 93.2%, DR Grading: 84.23%	RDR: 92.6%	RDR: 91.5%	RDR: 0.96	

Table 2. Characteristics and evaluation of DR grading methods. In this table, the methods that have no preprocessing or common preprocessing are mentioned. In addition to the abbreviations described earlier this table contains new abbreviations: Singapore integrated Diabetic Retinopathy Screening Program (SiDRP) between 2014 and 2015 (SiDRP 14-15), Singapore Malay Eye Study (SIMES), Singapore Indian Eye Study (SINDI), Singapore Chinese Eye Study (SCES), Beijing Eye Study (BES), African American Eye Study (AFEDS), Chinese University of Hong Kong (CUHK), and Diabetes Management Project Melbourne (DMP Melb) and Generative Adversarial Network (GAN).

Table 3: Classification-based studies in DR detection using a special preprocessing on fundus images for DR grading in ICDR scale.

Author, Year	Dataset	Pre-processing technique	Method	Accuracy
Datta, 2016 [141]	DRIVE, STARE, DIARETDB0, DIARETDB1	Yes, Contrast optimization	Image processing	NA
Lin, 2018 [142]	EyePACS	Yes, Convert to entropy images	DCNN	Original image: 81.8 % Entropy images: 86.1 %
Mukhopadhyay, 2018 [143]	Prasad Eye Institute, India	Yes, Local binary patterns	ML: Decision tree, KNN	KNN: 69.8 %
Pour, 2020 [144]	MESSIDOR 1,2, IDRID	Yes, CLAHE	DCNN: EfficientNet-B5	NA
Ramchandre, 2020 [145]	APTOS 2019	Yes, Image augmentation with AUGMIX	DCNN: EfficientNetb3, SEResNeXt32x4d	EfficientNetb3: 91.4 % SEResNeXt32x4d: 85.2 %
Shankar, 2020 [85]	MESSIDOR 1	Yes, CLAHE	DCNN: Hyperparameter Tuning Inception-v4 (HPTI-v4)	99.5 %
Bhardwaj, 2021 [146]	DRIVE, STARE, MESSIDOR 1, DIARETDB1, IDRID, ROC	Yes, Image contrast enhancement and OD localization	DCNN: InceptionResNet v2	93.3 %
Bilal, 2021 [16]	IDRID	Yes, Adaptive histogram equalization and contrast stretching	ML: SVM + KNN + Binary Tree	98.1 %
Eloumi, 2021 [147]	DIARETDB1	Yes, Sptic disk location, fundus image partitioning	ML: SVM, RF, KNN	98.4 %

AHE: Adaptive Histogram Equalization, CLAHE: Contrast Limited Adaptive Histogram Equalization.

Table 4: Classification-based studies in DR detection using OCT and OCTA.

Author, Year	Dataset	Grading details	Preprocessing	Method	Accuracy	Sensitivity	Specificity	AUC
Eladawi, 2018 [148]	OCTA images, University of Louisville, USA	Detect DR	Yes	ML: Vessel segmentation, Local feature extraction, SVM	97.3%	97.9%	96.4%	0.97
Islam, 2019 [149]	Kermani OCT dataset	NA	Yes	DCNN: DenseNet 201	98.6%	0.986	0.995	NA
Le, 2020 [150]	Private OCTA dataset	Grade DR	No	DCNN: VGG16	87.3 %	83.8 %	90.8 %	0.97
Sandhu, 2020 [74]	OCT. OCTA, clinical and demographical data, University of Louisville clinical center, USA	Detect mild and moderate DR	Yes	ML: RF	96.0%	100.0%	94.0%	0.96
Liu, 2021 [76]	Private OCTA dataset	Detect DR	Yes	Logistic Regression (LR), LR regularized with the elastic net (LR-EN), SVM and XGBoost	LR-EN: 80.0%	LR-EN: 82.0%	LR-EN: 84.0%	LR-EN: 0.83

### 3.3. Diabetic retinopathy lesion segmentation

The state-of-the-art DR diagnosis machines [66,67,151] identify referable DR identification without taking lesion information into account. Therefore, their predictions lack clinical interpretation, albeit their high accuracy. This black box nature is the major problem that makes the DCNNs unsuitable for clinical application[86,152,153] and has made the topic of eXplainable AI (XAI) of major importance [153]. Recently, the visualization techniques such as gradient-based XAI have been widely used for evaluating networks. However, these methods with generic heatmaps only highlight the major contributing lesions

and hence are not suitable for detection of DR with multiple lesions and severity. Thus, some studies focused on the lesion based DR detection instead. In general, we found 20 papers that do segmentation of the lesions such as MA (10 articles), Ex (9 articles) and IHE, VHE, PHE, IRMA, NV, CWS. In the following sections we discuss the general segmentation approach. The implementation details of each article are accessible in Tables 5 and 6 based on its imaging type.

### **3.3.1. Machine learning and un-machine learning approaches**

In general, using ML methods with high processing speed, low computational cost and interpretable decisions are preferred to DCNNs. However, the automatic detection of subtle lesions such as MA did not reach acceptable values. In this review we collected 2 pure ML-involved models and 6 un-ML methods. As reported in a study of Ali Shah 2016 [154] that detects MA with color, Hessian and curvelet-based feature extraction which achieved a SE of 48.2 %. Huang 2018 [155] focused on localizing NV through using Extreme Learning Machine (ELM). This study applied Standard deviation, Gabor, differential invariant and anisotropic filters for this purpose and with the final classifier applying ELM. This network performed as well as a SVM with lower computational time (6111 s vs 6877 s) with a PC running Microsoft Windows 7 operating system with a Pentium Dual-Core E5500 CPU and 4 GB memory. For the segmentation task, the preprocessing step had a fundamental rule which had a direct effect on the outputs. The preprocessing techniques varied depending on the lesion type and dataset quality. [Orlando 2018] applied a combination of DCNN and the manually designed features based on illumination correction, CLAHE contrast enhancement and color equalization. Then this high dimensionality feature vector was fed into a RF classifier to detect lesions and achieved an AUC score 0.93 which is comparable with some DCNN models [81,136,140].

Some studies used un-ML methods for detection of exudates such as that by Kaur et al 2018 [156] who proposed a pipeline consisting of vessel and optic disk removal and used a dynamic thresholding method for detection of CWS and Ex. Prior to this study, Imani et al 2016 [157] also did the same process with the focus on Ex with a smaller dataset. In their study they employed additional morphological processing and smooth edge removal to reduce the detection of CWS as Ex. This article reported the SE and SP of 89.1 % and 99.9 % and had almost similar performance compared to Kaur's results with 94.8 %, and 99.8 % for SE and SP respectively. Further description of the recent studies on lesion segmentation with ML approach can be found in Table 5 and 6.

### 3.3.2. Deep learning approaches

Recent works show that DCNNs can produce promising results in automated DR lesion segmentation. DR lesion segmentation is mainly focused on fundus imaging. However, some studies apply a combination of fundus and OCT. Holmberg 2020 [158] proposed a retinal layer extraction pipeline to measure retinal thickness with Unet. Furthermore, Yukun Guo et al 2018[159] applied DCNNs for avascular zone segmentation from OCTA images and received the accuracy of 87.0 % for mild to moderate DR and 76.0 % for severe DR.

Other studies mainly focus on DCNNs applied to fundus images which give a clear view of existing lesions on the surface of retina. Other studies such as Lam et al 2018[160] deployed state of art DCNNs to detect existence of DR lesions in image patches using AlexNet, ResNet, GoogleNet, VGG16 and Inception v3 achieving 98.0 % accuracy on a subset of 243 fundus images obtained from EyePACS. Wang et al 2021[26] also applied Inception v3 as the feature map in combination with FCN 32s as the segmentation part. They reported SE values of 60.7 %, 49.5 %, 28.3 %, 36.3 %, 57.3 %, 8.7 %, 79.8 % and 0.164 over PHE, Ex, VHE, NV, CWS, FIP, IHE, MA respectively. Quelled et al 2017[81] focused on four lesions CWS, Ex, HE and MA using a predefined DCNN architecture named o-O solution and reported the values of 62.4 %, 52.2 %, 44.9 % and 31.6 % over CWS, Ex, HE and MA for SE respectively which shows slightly better performance for CWS and Ex than Wang et al 2021[139]. Considerably better for MA than Wang et al 2021[139]. On the other hand, Wang et al performed better in HE detection. Further details of these article and others can be found in the Tables 5 and 6.

Table 5: Segmentation-based studies in DR detection using fundus images.

Author, Year	Dataset	Considered lesions	Preprocessing	Segmentation method	Sensitivity/ Specificity	AUC
Imani, 2016 [157]	DIARETDB1, HEI-MED, eOphta	Ex	Yes	Dynamic decision thresholding, morphological feature extraction, smooth edge removal	89.01%/ 99.93%	0.961
Shah, 2016 [154]	ROC	MA	Yes	Curvelet transform and rule-based classifier	48.2 %/ NA	NA
Quelled, 2017 [81]	EyePACS, eOphta, DIARETDB1	CWS, Ex, HE, MA	Yes	DCNN: o-O solution	DIARETDB1: CWS: 62.4%/ NA Ex: 55.2% / NA HE: 44.9% / NA MA: 31.6%/ NA	EyePACS: 0.955
Benzamin, 2018 [161]	IDRID	Ex	Yes	DCNN	98.29%/ 41.35%	ACC: 96.6%
Huang, 2018 [155]	MESSIDOR 1, DIARETDB0,1	NV	Yes	ELM	NA/ NA	ACC: 89.2%
Kaur, 2018 [156]	STARE, eOphta, MESSIDOR 1, DIARETDB1, private dataset	Ex, CWS	Yes	Dynamic decision thresholding	94.8%/ 99.80%	ACC: 98.43%

Lam, 2018 [160]	EyePACS, eOphtha	Ex, MA, HE, NV	NA	DCNN: AlexNet, VGG16, GoogleNet, ResNet, and Inception-v3	NA/ NA	EyePACS:0.99 ACC:98.0 %
Orlando,2018 [162]	eOphtha, DIARETDB1, MESSIDOR 1	MA, HE	Yes	ML: RF	NA/ NA	0.93
Eftekhari, 2019 [163]	ROC, eOphtha	MA	Yes	DCNN: Two level CNN, thresholded probability map	NA/ NA	ROC: 0.660
Wu, 2019 [164]	HRF	Blood vessels, optic disc and other regions	Yes	DCNN: AlexNet, GoogleNet, Resnet50, VGG19	NA/ NA	AlexNet: 0.94 ACC: 95.45%
Yan, 2019 [165]	IDRID	Ex, MA, HE, CWS	Yes	DCNN: Global and local Unet	NA/ NA	Ex:0.889 MA:0.525 HE: 0.703 CWS:0.679 ACC: 97.8%
Qiao, 2020 [166]	IDRID	MA	Yes	DCNN	98.4%/ 97.10%	
Wang, 2021 [140]	EyePACS, images from Peking Union Medical College Hospital	Detect RDR with lesion-based segmentation of PHE, VHE, NV, CWS, FIP, IHE, Ex, MA	No	DCNN: Inception v3 and FCN 32s	PHE: 60.7% / 90.9% Ex: 49.5% / 87.4% VHE: 28.3% / 84.6% NV: 36.3% / 83.7% CWS: 57.3% / 80.1% FIP: 8.7% / 78.0% IHE: 79.8% / 57.7% MA: 16.4%/ 49.8%	NA
Wei, 2021 [61]	EyePACS	MA, IHE, VHE, PHE, Ex, CWS, FIP, NV	Yes	DCNN: Transfer learning from Inception v3	NA/ NA	NA
Xu, 2021 [167]	IDRID	Ex, MA, HE, CWS	Yes	DCNN: Enhanced Unet named FFUnet	Ex:87.55%/ NA MA:59.33% / NA HE:73.42% / NA CWS:79.33%/ NA	IOU: Ex:0.84 MA:0.56 HE:0.73 CWS:0.75

ICDR scale: International Clinical Diabetic Retinopathy scale, RDR: Referable DR, vtDR: vision threatening DR, PDR: Proliferative DR, NPDR: Non-Proliferative DR, MA: Microaneurysm, Ex: hard Exudate, CWS: Cotton Wool Spot, HE: Hemorrhage, FIP: Fibrous Proliferation, VHE: Vitreous Hemorrhage, PHE: Preretinal Hemorrhage, NV: Neovascularization.

Table 6: Segmentation-based studies in DR detection using OCT, OCTA images.

Author, Year	Dataset	Considered lesions	Pre-processing	Segmentation method	Sensitivity	Specificity	AUC
Guo, 2018 [159]	UW-OCTA private dataset	Avascular area	Yes	DCNN	Control: 100.0% Diabetes without DR: 99.0% Mild to moderate DR: 99.0% Severe DR: 100.0%	Control: 84.0% Diabetes without DR: 77.0% Mild to moderate DR: 85.0% Severe DR: 68.0%	ACC: Control: 89.0% Diabetes without DR: 79% Mild to moderate DR: 87% Severe DR: 76.0%
EITanboly, 2018 [168]	OCT and OCTA images of University of Louisville	12 different retinal layers & segmented OCTA plexuses	No	SVM	NA	NA	ACC: 97.0%
EITanboly, 2018 [169]	SD-OCT images of Kentucky Lions Eye Center	12 distinct retinal layers	Yes	Statistical analysis and extraction of features such as tortuosity, reflectivity, and thickness for 12 retinal layers	NA	NA	ACC:73.2%
Sandhu, 2018 [168]	OCT images of University of Louisville, USA	12 layers; quantifies the reflectivity, curvature, and thickness	Yes	DCNN: 2 Stage deep CNN	92.5%	95.0%	ACC: 93.8%
Holmberg, 2020 [158]	OCT from Helmholtz Zentrum München, Fundus from EyePACS	Segment retinal thickness map, Grade DR based on ICDR scale	No	DCNN: On OCT: Retinal layer segmentation with Unet On fundus: Self supervised learning, ResNet50	NA	NA	IOU: on OCT: 0.94

#### 4. Conclusion

Recent studies for DR detection are mainly focused on automated methods known as CAD systems. In the scope of CAD system for DR there are two major approaches known as first classification and staging DR severity and second segmentation of lesions such as MA, HE, Ex, CWS associated with DR.

The DR databases are categorized to public databases (36 out of 43) and private databases (7 out of 43). These databases contain fundus and OCT retinal images and among these two imaging modalities fundus photos are used in 86.0 % of the published studies. Several public large fundus datasets are available online. The images might have been taken with different systems that affect image quality. Furthermore, some of the image-wise DR labels can be erroneous. The image databases that provide lesion annotations constitute only a small portion of the databases that require considerable resources for pixel-wise annotation. Hence, some of them contain fewer images than image-wise labeled databases. Furthermore, Lesion annotations requires intra-annotator agreement and high annotation precision. These factors make the dataset error sensitive, and its quality evaluation might become complicated.

The DR classification needs a standard grading system validated by clinicians. The ETDRS is the gold standard grading system proposed for DR progression grading but since this grading type needs fine detail evaluation and access to all 7 FOV fundus images, these issues make the use of ETDRS limited. There ICDR with less precise scales is applicable for 1 FOV images to detect the DR severity levels.

The classification and grading DR images can be divided to two main approaches, namely ML-based and DL-based classification. The ML-based DR detection has considerably better performance than grading using the ICDR scale which needs to extract higher-level features associated with each level of DR [55,70]. The evaluation results also proved that the DCNN architectures can achieve higher performance scores when large databases are used [71]. There is a trade-off between the performance on one side and the architecture complexity, processing time and the lack of interpretability over the network's decisions and extracted features on the other side. Thus, some recent works have proposed semi-DCNN models containing both DL based and ML-based models acting as classifier or feature extractor [70,71]. The use of regularization techniques is another solution to reduce the complexity of DCNN models [81].

The second approach for CAD-related studies in DR is pixel-wise lesion segmentation or image-wise lesion detection. The main lesions of DR are MA, Ex, HE, CWS. These lesions have different detection difficulty which directly affects the performance of proposed pipeline. Among these lesions the annotation of MA is more challenging [26,167]. Since this lesion is difficult to detect and is the main sign of DR in early stages,

some studies focused on the pixel-wise segmentation of this lesion with DCNNs and achieved high enough scores [166]. Although some of the recent DCNN- based works exhibit high performance in term of the standard metrics, the lack of interpretability may not be sufficiently valid for real-life clinical applications. This interpretability brings into the picture the concept of explainable AI or XAI. Explainability studies aim to show the features that influence the decision of a model the most. Singh et al [170] have reviewed the currently used explainability methods. There is also the need for a large fundus database with high precision annotation of all associated DR lesions to help in designing more robust and pipelines with high performance.

**Author Contributions:** Conceptualization V.L. and J.J.B.; methodology, V.L. and J.J.B.; dataset constitution H.K. and A.S.; writing-original draft preparation H.K, A.S. and J.J.B; writing-review and editing V.L; project administration V. L. and J. J. B. All authors have read and agreed to the published version of the manuscript.

**Funding:** This research was partly supported by a DISCOVERY grant to VL from the Natural Sciences and Engineering Research Council of Canada.

**Institutional Review Board Statement:** Not applicable. Study doesn't involve humans or animals.

**Informed Consent Statement:** Study didn't involve humans or animals and therefore informed consent is not applicable.

**Data Availability Statement:** This is review of the published articles, and all the articles are publically available.

**Acknowledgments:** A. S. acknowledges MITACS, Canada for the award of a summer internship.

**Conflicts of Interest:** The authors have no conflicts of interest.

## References

1. Bourne, R.R.A.; Steinmetz, J.D.; Saylan, M.; Mersha, AM, Weldemariam, A.H, et al. Causes of blindness and vision impairment in 2020 and trends over 30 years, and prevalence of avoidable blindness in relation to VISION 2020: The Right to Sight: An analysis for the Global Burden of Disease Study. *Lancet Glob Heal.* **2021**,*9*,e144–60.
2. Oh, K.; Kang, H.M.; Leem, D.; Lee, H.; Seo, K.Y.; et al. Early detection of diabetic retinopathy based on deep learning and ultra-wide-field fundus images. *Sci Rep.* **2021**,*11*,1897. DOI:10.1038/s41598-021-81539-3

3. Grading Diabetic Retinopathy from Stereoscopic Color Fundus Photographs-An Extension of the Modified Airlie House Classification: ETDRS Report Number 10. *Ophthalmology*. **1991**,98,786-806.
4. Horton, M.B.; Brady, C.J.; Cavallerano, J.; Abramoff, M.; Barker, G., et al. Practice Guidelines for Ocular Telehealth-Diabetic Retinopathy, Third Edition. *Telemed J E Health*. **2020**;26,495–543.
5. Solomon, S.D.; Goldberg, M.F. ETDRS Grading of Diabetic Retinopathy: Still the Gold Standard? *Ophthalmic Res*. **2019**, 62, 190–5.
6. Wilkinson, C.P.; Ferris, F.L.; Klein, R.E.; Lee, P.P.; Agardh, C.D., et al. Proposed International Clinical Diabetic Retinopathy and Diabetic Macular Edema Disease Severity Scales. *Ophthalmology*. **2003**,110,1677–82.
7. Rajalakshmi, R.; Prathiba, V.; Arulmalar, S.; Usha, M. Review of retinal cameras for global coverage of diabetic retinopathy screening. *Eye* **2021**, 35,162–72.
8. Qureshi, I.; Ma, J.; Abbas, Q. Recent development on detection methods for the diagnosis of diabetic retinopathy. *Symmetry* **2019**, 11,749. [www.mdpi.com/journal/symmetry](http://www.mdpi.com/journal/symmetry).
9. Chandran, A.; Mathai, A. *Diabetic Retinopathy for the Clinician*. Jaypee Brothers: Chennai, India, **2009**; Vol 1, Chapter 7, p 79.
10. Ludwig, C.A.; Perera, C.; Myung, D.; Greven, M.A.; Smith, S.J., et al. Automatic identification of referral-warranted diabetic retinopathy using deep learning on mobile phone images. *Transl Vis Sci Technol*. **2020**, 9, 1–7.
11. Hsu, W.; Pallawala, P.M.D.S.; Lee, M.L.; Eong, K.G.A. The role of domain knowledge in the detection of retinal hard exudates. *Proc IEEE Comput Soc Conf Comput Vis Pattern Recognit*. 2001;2.
12. Teo, Z.L.; Tham, Y-C.; Yu, M.; Chee, M.L.; Rim, T.H., et al. Global Prevalence of Diabetic Retinopathy and Projection of Burden through 2045. *Ophthalmology*. **2021**, 1–12. DOI:10.1016/j.ophtha.2021.04.027
13. Jeba Derwin, D.; Tamil Selvi, S.; Jeba Singh, O.; Priestly Shan, B. A novel automated system of discriminating Microaneurysms in fundus images. *Biomed Signal Process Control*. **2020**, 58, 101839. DOI:10.1016/j.bspc.2019.101839
14. Sivaprasad, S.; Raman, R.; Conroy, D.; Mohan, V.; Wittenberg, R, et al. The ORNATE India Project: United Kingdom–India Research Collaboration to tackle visual impairment due to diabetic retinopathy. *Eye*. **2020**, 34, 1279–86.
15. Majumder, S.; Elloumi, Y.; Akil, M.; Kachouri, R.; Kehtarnavaz, N. A deep learning-based smartphone app for real-time detection of five stages of diabetic retinopathy. In *Real-Time Image Processing and Deep Learning 2020*. **2020**,11401, p1140106. DOI:10.1117/12.2557554.
16. Bilal, A.; Sun, G.; Li, Y.; Mazhar, S.; Khan, AQ. Diabetic Retinopathy Detection and Classification Using Mixed Models for a Disease Grading Database. *IEEE Access*. **2021**,9,23544–53.
17. Leopold, H.; Zelek J.; Lakshminarayanan, V. *Deep Learning Methods Applied to Retinal Image Analysis in Signal Processing and Machine Learning for Biomedical Big Data*. In: CRC Press. E.Sejdic and T.Falk; **2018**. p 329.
18. Sengupta, S.; Singh, A.; Leopold, HA.; Gulati, T.; Lakshminarayanan, V. Ophthalmic diagnosis using deep learning with fundus images – A critical review. *Artif Intell Med*. **2020**, 102, 01758.
19. Leopold, H.; Sengupta, S.; Singh, A.; Lakshminarayanan, V. *Deep Learning on Optical Coherence Tomography for Ophthalmology, in State-of-the-art in neural networks*. In Academic Press; Elsevier, New York, USA, **2021**.

20. Hormel, TT.; Hwang, TS.; Bailey, ST.; Wilson, DJ.; Huang, D., et al. Artificial intelligence in OCT angiography. *Prog Retin Eye Res.* **2021**, 100965. DOI:10.1016/j.preteyeres.2021.100965
21. Methley, AM.; Campbell, S.; Chew-Graham, C.; McNally, R.; Cheraghi-Sohi, S. PICO, PICOS and SPIDER: A comparison study of specificity and sensitivity in three search tools for qualitative systematic reviews. *BMC Health Serv Res.* **2014**, 14,1-10.
22. Moher, D.; Liberati, A.; Tetzlaff, J.; Altman, DG.; Altman, D., et al. Preferred reporting items for systematic reviews and meta-analyses: The PRISMA statement. *PLoS Med.* **2009**,6, e1000097.
23. Khan, SM.,; Liu, X.; Nath, S.; Korot, E.; Faes, L., et al. A global review of publicly available datasets for ophthalmological imaging: barriers to access, usability, and generalisability. *Lancet Digit Heal.* **2021**,3,e51–66. DOI:10.1016/S2589-7500(20)30240-5
24. Chetoui, M.; Akhloufi, MA. Explainable end-to-end deep learning for diabetic retinopathy detection across multiple datasets. *J Med Imaging.* **2020**, 7,1–25.
25. Somaraki, V.; Broadbent, D.; Coenen, F.; Harding, S. Finding temporal patterns in noisy longitudinal data: A study in diabetic retinopathy. *Advances in Data Mining. Applications and Theoretical Aspects Lecture Notes in Computer Science.* **2010**; Vol 6171, pp:418–31.
26. Zhou, Y.; Wang, B.; Huang, L.; Cui, S.; Shao, L. A Benchmark for Studying Diabetic Retinopathy: Segmentation, Grading, and Transferability. *IEEE Trans Med Imaging.* **2021**,40. DOI:
27. Drive-grand challenge official website, Available online:<https://drive.grand-challenge.org/> Accessed on 23/5/2021.
28. Kauppi, T.; Kalesnykiene, V.; Kamarainen, J.; Lensu, L.; Sorri, I. DIARETDB0 : Evaluation Database and Methodology for Diabetic Retinopathy Algorithms. *Mach Vis Pattern Recognit Res Group, Lappeenranta Univ Technol Finland.* **2006**;1–17. [http://www.suue.edu/~sumbaug/RetinalProjectPapers/Diabetic Retinopathy Image Database Information.pdf](http://www.suue.edu/~sumbaug/RetinalProjectPapers/Diabetic_Retinopathy_Image_Database_Information.pdf) Accessed on 25/5/2021.
29. Kauppi, T.; Kalesnykiene, V.; Kamarainen, JK.; Lensu, L.; Sorri, I, et al. The DIARETDB1 diabetic retinopathy database and evaluation protocol. *BMVC 2007 - Proc Br Mach Vis Conf 2007.* **2007**;1–18.
30. Hsieh, YT.; Chuang, LM.; Jiang, Y Der.; Chang, TJ.; Yang, CM, et al. Application of deep learning image assessment software VeriSee™ for diabetic retinopathy screening. *J Formos Med Assoc.* **2021**, 120, 165–71. DOI:10.1016/j.jfma.2020.03.024.
31. Giancardo, L.; Meriaudeau, F.; Karnowski, TP.; Li, Y.; Garg, S, et al. Exudate-based diabetic macular edema detection in fundus images using publicly available datasets. *Med Image Anal.* **2012**, 16, 216–26.
32. Alipour, SHM.; Rabbani, H.; Akhlaghi, M.; Dehnavi, AM.; Javanmard, SH. Analysis of foveal avascular zone for grading of diabetic retinopathy severity based on curvelet transform. *Graefe's Arch Clin Exp Ophthalmol.* **2012**, 250, 1607–14.
33. Hajeb Mohammad Alipour, S.; Rabbani, H.; Akhlaghi, MR. Diabetic retinopathy grading by digital curvelet transform. *Comput Math Methods Med* 2012. **2012**, 1-11.
34. Esmaeili, M.; Rabbani, H.; Dehnavi, AM.; Dehghani, A. Automatic detection of exudates and optic disk in retinal images using curvelet transform. *IET Image Process.* **2012**, 6, 1005–13.
35. Prentasic, P.; Loncaric, S.; Vatavuk, Z.; Bencic, G.; Subasic, M, et al. Diabetic retinopathy image database(DRiDB): A new database for diabetic retinopathy screening programs research. *Int Symp Image Signal Process Anal ISPA.* **2013**, 711, 711–6.

36. Decencière, E.; Cazuguel, G.; Zhang, X.; Thibault, G.; Klein, JC, et al. TeleOphta: Machine learning and image processing methods for teleophthalmology. *Irbm*. **2013**, 34,196–203.
37. Odstrcilik, J.; Kolar, R.; Budaj, A.; Hornegger, J.; Jan, J, et al. Retinal vessel segmentation by improved matched filtering: Evaluation on a new high-resolution fundus image database. *IET Image Process*. **2013**,7, 373–83.
38. Hu, Q.; Abràmoff, MD.; Garvin, MK. Automated Separation of Binary Overlapping Trees in Low-Contrast Color Retinal Images. In: Mori K., Sakuma I., Sato Y., Barillot C., Navab N. (eds) Medical Image Computing and Computer-Assisted Intervention – MICCAI 2013. MICCAI **2013**. Lecture Notes in Computer Science, vol 8150. Springer, Berlin, Heidelberg. DOI:10.1007/978-3-642-40763-5\_54
39. Pires, R.; Jelinek, HF.; Wainer, J.; Valle, E.; Rocha, A. Advancing bag-of-visual-words representations for lesion classification in retinal images. *PLoS One*. **2014**, 9, e96814. DOI:10.1371/journal.pone.0096814
40. Sevik, U.; Köse, C.; Berber, T.; Erdöl, H. Identification of suitable fundus images using automated quality assessment methods. *J Biomed Opt*. **2014**, 19, 046006.
41. Hajeb Mohammad Alipour, S.; Rabbani, H.; Akhlaghi, M. A new combined method based on curvelet transform and morphological operators for automatic detection of foveal avascular zone. *Signal, Image Video Process*. **2014**, 8, 205–22.
42. Decencière, E.; Zhang, X.; Cazuguel, G.; Laÿ, B.; Cochener, B, et al. Feedback on a publicly distributed image database: The Messidor database. *Image Anal Stereol*. **2014**, 33, 231–4.
43. Bala, MP.; Vijayachitra, S. Early detection and classification of microaneurysms in retinal fundus images using sequential learning methods. *Int J Biomed Eng Technol*. **2014**, 15, 128–43.
44. Srinivasan, PP.; Kim, LA.; Mettu, PS.; Cousins, SW.; Comer, GM, et al. Fully automated detection of diabetic macular edema and dry age-related macular degeneration from optical coherence tomography images. *Biomed Opt Express*. **2014**, 5, 3568.
45. Kaggle.com, Available online: <https://www.kaggle.com/c/diabetic-retinopathy-detection/data> Accessed on 26/05/2021.
46. People.duke.edu website, available online: <http://people.duke.edu/~sf59/software.html> Accessed on 26/05/2021.
47. Holm, S.; Russell, G.; Nourrit, V.; McLoughlin, N. DR HAGIS—a fundus image database for the automatic extraction of retinal surface vessels from diabetic patients. *J Med Imaging*. **2017**, 4, 014503.
48. Takahashi, H.; Tampo, H.; Arai, Y.; Inoue, Y.; Kawashima, H. Applying artificial intelligence to disease staging: Deep learning for improved staging of diabetic retinopathy. *PLoS One*. **2017**, 12, 6, 1–11.
49. Rotterdam Ophthalmic Data Repository. re3data.org. Available online: <https://www.re3data.org/repository/r3d100012445>. Accessed on: 22/06/2021.
50. Ting, DSW.; Cheung, CYL.; Lim, G.; Tan, GSW.; Quang, ND, et al. Development and validation of a deep learning system for diabetic retinopathy and related eye diseases using retinal images from multiethnic populations with diabetes. *JAMA*. **2017**, 318, 2211–23.
51. Porwal, P.; Pachade, S.; Kamble, R.; Kokare, M.; Deshmukh, G, et al. Indian diabetic retinopathy image dataset (IDRiD): A database for diabetic retinopathy screening research. *Data*. **2018**, 3, 1–8.

52. Gholami, P.; Roy, P.; Parthasarathy, MK.; Lakshminarayanan, V. OCTID: Optical coherence tomography image database. *Comput Electr Eng.* **2020**, *81*, 1–8.
53. Abdulla W, Chalakkal RJ. University of Auckland Diabetic Retinopathy (UoA-DR) Database-end user licence agreement. Available online: [https://auckland.figshare.com/articles/journal\\_contribution/UoA-DR\\_Database\\_Info/5985208](https://auckland.figshare.com/articles/journal_contribution/UoA-DR_Database_Info/5985208). Accessed on: 28/05/2021.
54. Kaggle.com. Available from: <https://www.kaggle.com/c/aptos2019-blindness-detection>. Accessed on: 23/05/2021.
55. Ali, A.; Qadri, S.; Mashwani, W.K.; Kumam, W.; Kumam, P, et al. Machine learning based automated segmentation and hybrid feature analysis for diabetic retinopathy classification using fundus image. *Entropy.* **2020**, *22*, 569.
56. Díaz, M.; Novo, J.; Cutrín, P.; Gómez-Ulla, F.; Penedo, M.G, et al Automatic segmentation of the foveal avascular zone in ophthalmological OCT-A images. *PLoS One.* **2019**,*14*,1–22.
57. ODIR-2019. Available from: <https://odir2019.grand-challenge.org/>. Accessed on 22/06/2021.
58. Li, T.; Gao, Y.; Wang, K.; Guo, S.; Liu, H.; Kang, H. Diagnostic assessment of deep learning algorithms for diabetic retinopathy screening. *Inf Sci (Ny).* **2019**, *501*, 511–22. DOI:10.1016/j.ins.2019.06.011
59. Li, F.; Liu, Z.; Chen, H.; Jiang, M.; Zhang, X.; Wu, Z. Automatic detection of diabetic retinopathy in retinal fundus photographs based on deep learning algorithm. *Transl Vis Sci Technol.* **2019**, *8*,4-4.
60. Benítez, V.E.; Matto, I.C.; Román, J.C.; Noguera, J.L.; García-Torres, M, et al. Dataset from fundus images for the study of diabetic retinopathy. *Data in Brief.* **2021**, Available from: <https://zenodo.org/record/4647952>
61. Wei, Q.; Li, X.; Yu, W.; Zhang, X.; Zhang, Y, et al. Learn to Segment Retinal Lesions and Beyond. *In: 2020 25<sup>th</sup> International Conference on Pattern Recognition (ICPR).* IEEE; **2021**,7403–10.
62. Noor-Ul-Huda, M.; Tehsin, S.; Ahmed, S.; Niazi, F.A.K.; Murtaza, Z. Retinal images benchmark for the detection of diabetic retinopathy and clinically significant macular edema (CSME). *Biomed Tech.* **2019**,*64*,297–307.
63. Ohsugi, H.; Tabuchi, H.; Enno, H.; Ishitobi, N. Accuracy of deep learning, a machine-learning technology, using ultra-wide-field fundus ophthalmoscopy for detecting rhegmatogenous retinal detachment. *Sci Rep.* **2017**,*7*,17–20. DOI:10.1038/s41598-017-09891-x
64. Abràmoff, M.D.; Lou, Y.; Erginay, A.; Clarida, W.; Amelon, R, et al. Improved automated detection of diabetic retinopathy on a publicly available dataset through integration of deep learning. *Investig Ophthalmol Vis Sci.* **2016**, *57*, 5200–6.
65. Kafieh, R.; Rabbani, H.; Hajizadeh, F.; Ommani, M. An accurate multimodal 3-D vessel segmentation method based on brightness variations on OCT layers and curvelet domain fundus image analysis. *IEEE Trans Biomed Eng.* **2013**, *60*,2815–23.
66. Gargeya, R.; Leng, T. Automated Identification of Diabetic Retinopathy Using Deep Learning. *Ophthalmology.* **2017**,*124*,1–8.
67. Gulshan, V.; Peng, L.; Coram, M.; Stumpe, M.C.; Wu, D, et al. Development and validation of a deep learning algorithm for detection of diabetic retinopathy in retinal fundus photographs. *JAMA - J Am Med Assoc.* **2016**,*316*,2402–10.
68. Abràmoff, M.D.; Lou, Y.; Erginay, A.; Clarida, W.; Amelon, R, et al. Improved automated detection of diabetic retinopathy on a publicly available dataset through integration of deep learning. *Investig Ophthalmol Vis Sci.* **2016**, *57*,5200–6.

69. Sahlsten, J.; Jaskari, J.; Kivinen, J.; Turunen, L.; Jaanio, E, et al. Deep Learning Fundus Image Analysis for Diabetic Retinopathy and Macular Edema Grading. *Sci Rep.* **2019**, *9*, 1–11.
70. Gadekallu, T.R.; Khare, N.; Bhattacharya, S.; Singh, S.; Maddikunta, P.K.R, et al. Early detection of diabetic retinopathy using pca-firefly based deep learning model. *Electron.* **2020**, *9*, 1–16.
71. Mansour, R.F. Deep-learning-based automatic computer-aided diagnosis system for diabetic retinopathy. *Biomed Eng Lett.* **2018**, *8*, 41–57.
72. Paradisa, R.H.; Sarwinda, D.; Bustamam, A.; Argyadiva, T. Classification of Diabetic Retinopathy through Deep Feature Extraction and Classic Machine Learning Approach. In: *2020 3<sup>rd</sup> International Conference on Information and Communications Technology, ICOIACT 2020.* **2020**, 377-381.
73. Elswah, D.K.; Elnakib, A.A.; El-Din Moustafa, H. Automated Diabetic Retinopathy Grading using Resnet. In: *National Radio Science Conference, NRSC, Proceedings.* **2020**, 248–54.
74. Sandhu, H.S.; Elmogy, M.; Taher Sharafeldein, A.; Elsharkawy, M.; El-Adawy, N, et al. Automated Diagnosis of Diabetic Retinopathy Using Clinical Biomarkers, Optical Coherence Tomography, and Optical Coherence Tomography Angiography. *Am J Ophthalmol.* **2020**, *216*, 201–6. DOI:10.1016/j.ajo.2020.01.016
75. Somasundaram, S.K.; Alli, P. A Machine Learning Ensemble Classifier for Early Prediction of Diabetic Retinopathy. *J Med Syst.* **2017**, *41*, 1-2.
76. Liu, Z.; Wang, C.; Cai, X.; Jiang, H.; Wang, J. Discrimination of Diabetic Retinopathy from Optical Coherence Tomography Angiography Images Using Machine Learning Methods. *IEEE Access.* **2021**, *9*, 51689–94.
77. Levenkova, A.; Kalloniatis, M.; Ly, A.; Ho, A.; Sowmya, A. Lesion detection in ultra-wide field retinal images for diabetic retinopathy diagnosis. In *Medical Imaging 2018: Computer-Aided Diagnosis*, International Society for Optics and Photonics. **2018**, 10575, p 1057531.
78. Narayanan, B.N.; Hardie, R.C.; De Silva, M.S.; Kueterman, N.K. Hybrid machine learning architecture for automated detection and grading of retinal images for diabetic retinopathy. *J Med Imaging.* **2020**, *7*, p 034501.
79. Rajalakshmi, R.; Subashini, R.; Anjana, R.M.; Mohan, V. Automated diabetic retinopathy detection in smartphone-based fundus photography using artificial intelligence. *Eye.* **2018**, *32*, 1138–44. DOI:10.1038/s41433-018-0064-9
80. Riaz, H.; Park, J.; Choi, H.; Kim, H.; Kim, J. Deep and densely connected networks for classification of diabetic retinopathy. *Diagnostics.* **2020**, *10*, 1–15.
81. Quellec G, Charrière K, Boudi Y, Cochener B, Lamard M. Deep image mining for diabetic retinopathy screening. *Med Image Anal.* 2017;39:178–93.
82. Sayres, R.; Taly, A.; Rahimy, E.; Blumer, K.; Coz, D, et al. Using a Deep Learning Algorithm and Integrated Gradients Explanation to Assist Grading for Diabetic Retinopathy. *Ophthalmology.* **2019**, *126*, 552–64. DOI:10.1016/j.ophtha.2018.11.016
83. Hua, C.H.; Huynh-The, T.; Kim, K.; Yu, S.Y.; Le-Tien, T, et al. Bimodal learning via trilogy of skip-connection deep networks for diabetic retinopathy risk progression identification. *Int J Med Inform.* **2019**, *132*, 103926. DOI:10.1016/j.ijmedinf.2019.07.005
84. Pao, S.I.; Lin, H.Z.; Chien, K.H.; Tai, M.C.; Chen, J.T.; Lin, G.M. Detection of Diabetic Retinopathy Using Bichannel Convolutional Neural Network. *J Ophthalmol.* **2020**. DOI:10.1155/2020/9139713

85. Shankar, K.; Sait, A.R.W.; Gupta, D.; Lakshmanaprabu, S.K.; Khanna, A, et al. Automated detection and classification of fundus diabetic retinopathy images using synergic deep learning model. *Pattern Recognit Lett.* **2020**,133,210–6. DOI:10.1016/j.patrec.2020.02.026
86. Singh, A.; Sengupta, S.; Lakshminarayanan, V. Explainable deep learning models in medical image analysis. *J Imaging.* **2020**, 6, 1–19.
87. Singh, A.; Sengupta, S.; Rasheed, M.A.; Jayakumar, V.; Lakshminarayanan, V. Uncertainty aware and explainable diagnosis of retinal disease. *In Medical Imaging 2021: Imaging Informatics for Healthcare, Research, and Applications.* **2021**, 11601, 116010J. International Society for Optics and Photonics.
88. Singh, A.; Jothi Balaji, J.; Rasheed, M.A.; Jayakumar, V.; Raman, R.; Lakshminarayanan, V. Evaluation of Explainable Deep Learning Methods for Ophthalmic Diagnosis. *Clin Ophthalmol.* **2021**, 15,2573–81.
89. Keel, S.; Wu, J.; Lee, P.Y.; Scheetz, J.; He, M. Visualizing Deep Learning Models for the Detection of Referable Diabetic Retinopathy and Glaucoma. *JAMA Ophthalmol.* **2019**, 137, 288–92.
90. Chandrakumar, T.; R, Kathirvel. Classifying Diabetic Retinopathy using Deep Learning Architecture. *Int J Eng Res.* **2016**, V5,19–24.
91. Colas, E.; Besse, A.; Orgogozo, A.; Schmauch, B.; Meric, N, et al. Deep learning approach for diabetic retinopathy screening. *Acta Ophthalmol.* **2016**, 94; DOI:10.1111/j.1755-3768.2016.0635.
92. Wong, T.Y.; Bressler, N.M., CY, W.; SB, B.; NM, B. Artificial Intelligence With Deep Learning Technology Looks Into Diabetic Retinopathy Screening. *JAMA.* **2016**, 304, 649–56; DOI:10.1001/jama.2016.17563
93. Wang, Z.; Yin, Y.; Shi, J.; Fang, W.; Li, H, et al. Zoom-in-net: Deep mining lesions for diabetic retinopathy detection. *International Conference on Medical Image Computing and Computer-Assisted Intervention.* **2017**, 10435 LNCS, 267–75.
94. Benson, J.; Maynard, J.; Zamora, G.; Carrillo, H.; Wigdahl, J, et al. Transfer learning for diabetic retinopathy. *Image Processing,* **2018**, 70, 105741Z.
95. Chakrabarty, N. A Deep Learning Method for the detection of Diabetic Retinopathy. *2018 5th IEEE Uttar Pradesh Section International Conference on Electrical, Electronics and Computer Engineering (UPCON).* **2018**, 1-5.
96. Costa, P.; Galdran, A.; Smailagic, A.; Campilho, A. A Weakly-Supervised Framework for Interpretable Diabetic Retinopathy Detection on Retinal Images. *IEEE Access.* **2018**, 6, 18747–58.
97. Dai, L.; Fang, R.; Li, H.; Hou, X.; Sheng, B, et al. Clinical report guided retinal microaneurysm detection with multi-sieving deep learning. *IEEE Trans Med Imaging.* 2018, 37, 1149-61.
98. Dutta, S.; Manideep, B.C.S.; Basha, S.M.; Caytiles, R.D.; Iyengar, N.C.S.N. Classification of diabetic retinopathy images by using deep learning models. *Int J Grid Distrib Comput.* **2018**, 11, 89–106.
99. Kwasigroch, A.; Jarzembinski, B.; Grochowski, M. Deep CNN based decision support system for detection and assessing the stage of diabetic retinopathy. *Int Interdiscip PhD Work IIPhDW.* **2018**, 111–6.
100. Islam, M.R.; Hasan, M.A.M.; Sayeed, A. Transfer Learning based Diabetic Retinopathy Detection with a Novel Preprocessed Layer. *IEEE Reg 10 Symp TENSYPMP 2020.* **2020**, 888–91.
101. Zhang, S.; Wu, H.; Wang, X.; Cao, L.; Schwartz, J, et al. The application of deep learning for diabetic retinopathy prescreening in research eye-PACS. *Imaging Informatics for Healthcare, Research, and Applications.* **2018**, 10579, 1057913.

102. Fang, M.; Zhang, X.; Zhang, W.; Xue, J.; Wu, L. Automatic classification of diabetic retinopathy based on convolutional neural networks. *International Conference on Image and Video Processing, and Artificial Intelligence*. **2018**, 10836, 1083608.
103. Arcadu, F.; Benmansour, F.; Maunz, A.; Willis, J.; Haskova, Z, et al. Deep learning algorithm predicts diabetic retinopathy progression in individual patients. *npj Digit Med*. 2019, 2, 1-9; DOI:10.1038/s41746-019-0172-3
104. Bellemo, V.; Lim, Z.W.; Lim, G.; Nguyen, Q.D.; Xie, Y, et al. Artificial intelligence using deep learning to screen for referable and vision-threatening diabetic retinopathy in Africa: a clinical validation study. *Lancet Digit Heal*. **2019**, 1, 35–44; DOI:10.1016/S2589-7500(19)30004-4.
105. Chowdhury, M.M.H.; Meem, N.T.A. A Machine Learning Approach to Detect Diabetic Retinopathy Using Convolutional Neural Network. *Springer Singapore*. **2020**, 255–264; DOI:10.1007/978-981-13-7564-4\_23.
106. Govindaraj, V.; Balaji, M.; Mohideen, TA.; Mohideen, S.A.F.J. Eminent identification and classification of Diabetic Retinopathy in clinical fundus images using Probabilistic Neural Network. *IEEE Int Conf Intell Tech Control Optim Signal Process INCOS*, **2019**, 1-6.
107. Gulshan, V.; Rajan, R.P.; Widner, K.; Wu, D.; Wubbels, P, et al. Performance of a Deep-Learning Algorithm vs Manual Grading for Detecting Diabetic Retinopathy in India. *JAMA Ophthalmol*. **2019**, 137, 987–93.
108. Hathwar, S.B.; Srinivasa, G. Automated Grading of Diabetic Retinopathy in Retinal Fundus Images using Deep Learning. *Proc 2019 IEEE Int Conf Signal Image Process Appl ICSIPA 2019*. **2019**, 73–7.
109. He, J.; Shen, L.; Ai, X.; Li, X. Diabetic Retinopathy Grade and Macular Edema Risk Classification Using Convolutional Neural Networks. *2019 IEEE Int Conf Power, Intell Comput Syst ICPICS 2019*. **2019**, 463–6.
110. Jiang, H.; Yang, K.; Gao, M.; Zhang, D.; Ma, H, et al. An Interpretable Ensemble Deep Learning Model for Diabetic Retinopathy Disease Classification. *Proc Annu Int Conf IEEE Eng Med Biol Soc EMBS*. **2019**, 2045–8.
111. Li, X.; Hu, X.; Yu, L.; Zhu, L.; Fu, C.W, et al. CANet: Cross-Disease Attention Network for Joint Diabetic Retinopathy and Diabetic Macular Edema Grading. *IEEE Trans Med Imaging*. **2020**, 39, 1483–93.
112. Metan, A.C.; Lambert, A.; Pickering, M. Small Scale Feature Propagation Using Deep Residual Learning for Diabetic Retinopathy Classification. *2019 IEEE 4th Int Conf Image, Vis Comput ICIVC 2019*. **2019**, 392–6.
113. Nagasawa, T.; Tabuchi, H.; Masumoto, H.; Enno, H.; Niki, M, et al. Accuracy of ultrawide-field fundus ophthalmoscopy-assisted deep learning for detecting treatment-naïve proliferative diabetic retinopathy. *Int Ophthalmol*. **2019**, 39, 2153–9; DOI:10.1007/s10792-019-01074-z.
114. Qummar, S.; Khan, F.G.; Shah, S.; Khan, A.; Shamshirband, S, et al. A Deep Learning Ensemble Approach for Diabetic Retinopathy Detection. *IEEE Access*. **2019**, 7, 150530–9.
115. Bora, A.; Balasubramanian, S.; Babenko, B.; Virmani, S.; Venugopalan, S, et al. Predicting the risk of developing diabetic retinopathy using deep learning. *Lancet Digit Heal*. **2021**, 3, 10–9; DOI:10.1016/S2589-7500(20)30250-8.
116. Sengupta, S.; Singh, A.; Zelek, J.; Lakshminarayanan, V. Cross-domain diabetic retinopathy detection using deep learning. *Applications of Machine Learning*. 2019, 11139, 111390V.

117. Ting, D.S.W.; Cheung, C.Y.; Nguyen, Q.; Sabanayagam, C.; Lim, G, et al. Deep learning in estimating prevalence and systemic risk factors for diabetic retinopathy: a multi-ethnic study. *npj Digit Med.* **2019**, *2*, 1–8; DOI:10.1038/s41746-019-0097-x.
118. Zeng, X.; Chen, H.; Luo, Y.; Ye, W. Automated diabetic retinopathy detection based on binocular siamese-like convolutional neural network. *IEEE Access.* **2019**, *7*, 30744–53.
119. Araújo, T.; Aresta, G.; Mendonça, L.; Penas, S.; Maia, C, et al. DR|GRADUATE: Uncertainty-aware deep learning-based diabetic retinopathy grading in eye fundus images. *Med Image Anal.* **2020**, *63*, 101715.
120. Gadekallu, T.R.; Khare, N.; Bhattacharya, S.; Singh, S.; Maddikunta, P.K.R. Deep neural networks to predict diabetic retinopathy. *J Ambient Intell Humaniz Comput.* **2020**, 1-14.
121. Gayathri, S.; Krishna, A.K.; Gopi, V.P.; Palanisamy, P. Automated Binary and Multiclass Classification of Diabetic Retinopathy Using Haralick and Multiresolution Features. *IEEE Access.* **2020**, *8*, 57497–504.
122. Jiang, H.; Xu, J.; Shi, R.; Yang, K.; Zhang, D, et al. A Multi-Label Deep Learning Model with Interpretable Grad-CAM for Diabetic Retinopathy Classification. *Proc Annu Int Conf IEEE Eng Med Biol Soc EMBS.* **2020**, 1560–3.
123. Lands, A.; Kottarathil, A.J.; Biju, A.; Jacob, E.M.; Thomas, S. Implementation of deep learning based algorithms for diabetic retinopathy classification from fundus images. *Proc 4th Int Conf Trends Electron Informatics, ICOEI.* **2020**, 1028–32.
124. Memari, N.; Abdollahi, S.; Ganzagh, M.M.; Moghbel, M. Computer-assisted diagnosis (CAD) system for Diabetic Retinopathy screening using color fundus images using Deep learning. *2020 IEEE Student Conf Res Dev SCOREd.* **2020**, 69–73.
125. Patel, R.; Chaware, A. Transfer Learning with Fine-Tuned MobileNetV2 for Diabetic Retinopathy. In: *2020 International Conference for Emerging Technology (INCET).* *IEEE.* **2020**, 1–4.
126. Samanta, A.; Saha, A.; Satapathy, S.C.; Fernandes, S.L.; Zhang, Y.D. Automated detection of diabetic retinopathy using convolutional neural networks on a small dataset. *Pattern Recognit Lett.* **2020**, 135.
127. Serener, A.; Serte, S. Geographic variation and ethnicity in diabetic retinopathy detection via deep learning. *Turkish J Electr Eng Comput Sci.* **2020**, *28*, 664–78.
128. Shaban, M.; Ogur, Z.; Mahmoud, A.; Switala, A.; Shalaby, A, et al. A convolutional neural network for the screening and staging of diabetic retinopathy. *PLoS One.* **2020**, *15*, 1–13; DOI:10.1371/journal.pone.0233514
129. Singh, R.K.; Gorantla, R. DMenet: Diabetic Macular Edema diagnosis using Hierarchical Ensemble of CNNs. *PLoS One.* **2020**, *15*, 1–22; DOI:10.1371/journal.pone.0220677
130. Thota, N.B.; Umma Reddy, D. Improving the Accuracy of Diabetic Retinopathy Severity Classification with Transfer Learning. *Midwest Symp Circuits Syst.* **2020**, 1003–6.
131. Wang, X.N.; Dai, L.; Li, S.T.; Kong, H.Y.; Sheng, B, et al. Automatic Grading System for Diabetic Retinopathy Diagnosis Using Deep Learning Artificial Intelligence Software. *Curr Eye Res.* **2020**, *45*, 1550–5; DOI:10.1080/02713683.2020.1764975
132. Wang, J.; Bai, Y.; Xia, B. Simultaneous Diagnosis of Severity and Features of Diabetic Retinopathy in Fundus Photography Using Deep Learning. *IEEE J Biomed Heal Informatics.* **2020**, *24*, 3397–407.

133. Zhang, W.; Zhao, X.J.; Chen, Y.; Zhong, J.; Yi, Z. DeepUWF: An Automated Ultra-wide-field Fundus Screening System via Deep Learning. *IEEE J Biomed Heal Informatics*. **2020**, 2194, 1–9.
134. Abdelmaksoud, E.; El-Sappagh, S.; Barakat, S.; Abuhmed, T.; Elmogy, M. Automatic Diabetic Retinopathy Grading System Based on Detecting Multiple Retinal Lesions. *IEEE Access*. **2021**, 9, 15939–60.
135. Gangwar, AK.; Ravi, V. Diabetic Retinopathy Detection Using Transfer Learning and Deep Learning. *Advances in Intelligent Systems and Computing*. **2021**, 679–89.
136. He, A.; Li, T.; Li, N.; Wang, K.; Fu, H. CABNet: Category Attention Block for Imbalanced Diabetic Retinopathy Grading. *IEEE Trans Med Imaging*. **2021**, 40, 143–53.
137. Khan, Z.; Khan, F.G.; Khan, A.; Rehman, Z.U.; Shah, S, et al. Diabetic Retinopathy Detection Using VGG-NIN a Deep Learning Architecture. *IEEE Access*. **2021**, 9, 61408–16.
138. Saeed, F.; Hussain, M.; Aboalsamh, H.A. Automatic Diabetic Retinopathy Diagnosis Using Adaptive Fine-Tuned Convolutional Neural Network. *IEEE Access*. **2021**, 9, 41344–59.
139. Wang, Y.; Yu, M.; Hu, B.; Jin, X.; Li, Y, et al. Deep learning-based detection and stage grading for optimising diagnosis of diabetic retinopathy. *Diabetes Metab Res Rev*. **2021**, 37, e3445.
140. Wang, S.; Wang, X.; Hu, Y.; Shen, Y.; Yang, Z, et al. Diabetic Retinopathy Diagnosis Using Multichannel Generative Adversarial Network with Semisupervision. *IEEE Trans Autom Sci Eng*. **2021**, 18, 574–85.
141. Datta, NS.; Dutta, H.S.; Majumder, K. Brightness-preserving fuzzy contrast enhancement scheme for the detection and classification of diabetic retinopathy disease. *J Med Imaging*. **2016**, 3, 014502.
142. Lin, G.M.; Chen, M.J.; Yeh, C.H.; Lin, Y.Y.; Kuo, H.Y, et al. Transforming retinal photographs to entropy images in deep learning to improve automated detection for diabetic retinopathy. *J Ophthalmol*. **2018**, 2018.
143. Panigrahi, P.K.; Mukhopadhyay, S.; Pratiher, S.; Chhablani, J.; Mukherjee, S, et al. Statistical classifiers on local binary patterns for optical diagnosis of diabetic retinopathy. *Biophotonics: Photonic Solutions for Better Health Care VI*. 2018, 10685, 106852Y.
144. Momeni Pour, A.; Seyedarabi, H.; Abbasi Jahromi, S.H.; Javadzadeh A. Automatic detection and monitoring of diabetic retinopathy using efficient convolutional neural networks and contrast limited adaptive histogram equalization. *IEEE Access*. **2020**, 8, 136668–73.
145. Ramchandre, S.; Patil, B.; Pharande, S.; Javali, K.; Pande H. A Deep Learning Approach for Diabetic Retinopathy detection using Transfer Learning. *2020 IEEE Int Conf Innov Technol INOCON*. **2020**, 1-5.
146. Bhardwaj, C.; Jain, S.; Sood, M. Deep Learning–Based Diabetic Retinopathy Severity Grading System Employing Quadrant Ensemble Model. *J Digit Imaging*. **2021**, 1-18; DOI:10.1007/s10278-021-00418-5
147. Elloumi, Y.; Ben Mbarek, M.; Boukadida, R.; AKIL, M.; Bedoui, MH. Fast and accurate mobile-aided screening system of moderate diabetic retinopathy. *Thirteenth International Conference on Machine Vision*. **2021**, 11605, 93.
148. Eladawi, N.; Elmogy, M.; Fraiwan, L.; Pichi, F.; Ghazal, M, et al. Early Diagnosis of Diabetic Retinopathy in OCTA Images Based on Local Analysis of Retinal Blood Vessels and Foveal Avascular Zone. *Proc - Int Conf Pattern Recognit*. **2018**, 3886–91.

149. Islam, K.T.; Wijewickrema, S.; O'Leary, S. Identifying diabetic retinopathy from OCT images using deep transfer learning with artificial neural networks. *Proc - IEEE Symp Comput Med Syst.* **2019**, 281–6.
150. Le, D.; Alam, M.N.; Lim, J.I.; Chan, R.V.P.; Yao, X. Deep learning for objective OCTA detection of diabetic retinopathy. *Ophthalmic Technologies XXX.* **2020**, 11218, 112181P.
151. Gargeya, R.; Leng, T. Automated Identification of Diabetic Retinopathy Using Deep Learning. *Ophthalmology.* **2017**, 124, 962–9.
152. Singh, A.; Sengupta, S.; Mohammed, A.R.; Faruq, I.; Jayakumar, V, et al. What is the Optimal Attribution Method for Explainable Ophthalmic Disease Classification?. *Lecture Notes in Computer Science (including subseries Lecture Notes in Artificial Intelligence and Lecture Notes in Bioinformatics).* 2020. 21–31; DOI:10.1007/978-3-030-63419-3\_3
153. Singh, A.; Mohammed, A.R.; Zelek, J.; Lakshminarayanan, V. Interpretation of deep learning using attributions: application to ophthalmic diagnosis. *Applications of Machine Learning,* **2020**, 11511, 115110A.
154. Ali Shah, S.A.; Laude, A.; Faye, I.; Tang, T.B. Automated microaneurysm detection in diabetic retinopathy using curvelet transform. *J Biomed Opt.* **2016**, 21, 101404.
155. Huang, H.; Ma, H.; JW van Triest, H.; Wei, Y.; Qian, W. Automatic detection of neovascularization in retinal images using extreme learning machine. *Neurocomputing.* **2018**, 277, 218–27.
156. Kaur, J.; Mittal, D. A generalized method for the segmentation of exudates from pathological retinal fundus images. *Biocybern Biomed Eng.* 2018, 38, 27–53; DOI:10.1016/j.bbe.2017.10.003
157. Imani, E.; Pourreza, H.R. A novel method for retinal exudate segmentation using signal separation algorithm. *Comput Methods Programs Biomed.* **2016**, 133, 195–205; DOI:10.1016/j.cmpb.2016.05.016
158. Holmberg, O.G.; Köhler, N.D.; Martins, T.; Siedlecki, J.; Herold, T, et al. Self-supervised retinal thickness prediction enables deep learning from unlabelled data to boost classification of diabetic retinopathy. *Nat Mach Intell.* **2020**, 2, 719–26.
159. Guo, Y.; Camino, A.; Wang, J.; Huang, D.; Hwang, T.S, et al. MEDnet, a neural network for automated detection of avascular area in OCT angiography. *Biomed Opt Express.* 2018, 9, 5147.
160. Lam, C.; Yu, C.; Huang, L.; Rubin, D. Patches. Retinal lesion detection with deep learning using image patches. *Investigative ophthalmology & visual science.* **2018**, 59, 590-6.
161. Benzamin, A.; Chakraborty, C. Detection of hard exudates in retinal fundus images using deep learning. *2018 Jt 7th Int Conf Informatics, Electron Vis 2nd Int Conf Imaging, Vis Pattern Recognition, ICIEV-IVPR 2018.* **2019**, 465–9.
162. Orlando, J.I.; Prokofyeva, E.; del Fresno, M.; Blaschko, M.B. An ensemble deep learning based approach for red lesion detection in fundus images. *Computer Methods Programs Biomed.* **2018**, 153, 115–27.
163. Eftekhari, N.; Pourreza, H.R.; Masoudi, M.; Ghiasi-Shirazi, K.; Saeedi, E. Microaneurysm detection in fundus images using a two-step convolutional neural network. *Biomed Eng Online.* **2019**, 18, 1-16.
164. Wu, Q.; Cheddad, A. Segmentation-based Deep Learning Fundus Image Analysis. *2019 9th Int Conf Image Process Theory, Tools Appl IPTA 2019.* **2019**, 1–5.

165. Yan, Z.; Han, X.; Wang, C.; Qiu, Y.; Xiong, Z, et al. Learning mutually local-global u-nets for high-resolution retinal lesion segmentation in fundus images. *Proc - Int Symp Biomed Imaging*. **2019**, 597–600.
166. Qiao, L.; Zhu, Y.; Zhou, H. Diabetic Retinopathy Detection Using Prognosis of Microaneurysm and Early Diagnosis System for Non-Proliferative Diabetic Retinopathy Based on Deep Learning Algorithms. *IEEE Access*. **2020**, 8, 104292–302.
167. Xu, Y.; Zhou, Z.; Li, X.; Zhang, N.; Zhang, M, et al, FFU-Net: Feature Fusion U-Net for Lesion Segmentation of Diabetic Retinopathy. *Biomed Res Int*. **2021**.
168. Sandhu, H.S.; Eltanboly, A.; Shalaby, A.; Keynton, R.S; Schaal, S, et al. Automated diagnosis and grading of diabetic retinopathy using optical coherence tomography. *Investig Ophthalmol Vis Sci*. **2018**, 59, 3155–60.
169. ElTanboly, A.H.; Palacio, A.; Shalaby, A.M.; Switala, A.E.; Helmy, O, et al. An automated approach for early detection of diabetic retinopathy using SD-OCT images. *Front Biosci - Elit*. **2018**, 10, 197–207.
170. Singh, A.; Sengupta, S.; Rasheed, M.A.; Jayakumar, V.; Lakshminarayanan, V. Uncertainty aware and explainable diagnosis of retinal disease. *Medical Imaging 2021: Imaging Informatics for Healthcare, Research, and Applications*. **2021**, 11601, 116010J.